ELSEVIER

Tectonophysics 335 (2001) 81–109

TECTONOPHYSICS

www.elsevier.com/locate/tecto

Microstructure in linear elasticity and scale effects: a reconsideration of basic rock mechanics and rock fracture mechanics

George E. Exadaktylos[a,*], Ioannis Vardoulakis[b]

[a]*Department of Mineral Resources Engineering — Laboratory of Mine Design and Mechanics, Technical University of Crete, GR-73100, Chania, Greece*

[b]*Department of Engineering Science, National Technical University of Athens, GR-15773, Athens, Greece*

Abstract

An account on the role of higher order strain gradients in the mechanical behavior of elastic-perfectly brittle materials, such as rocks, is given that is based on a special grade-2 elasticity theory with surface energy as this was originated by Casal and Mindlin and further elaborated by the authors. The fundamental idea behind the theory is that the effect of the granular and polycrystalline nature of geomaterials (i.e. their microstructural features) on their macroscopic response may be modeled through the concept of volume cohesion forces, as well as surface forces rather than through intractable statistical mechanics concepts of the Boltzmann type. It is shown that the important phenomena of the localization of deformation in macroscopically homogeneous rocks under uniform tractions and of dependence of rock behavior on the specimen's dimensions, commonly known as size or scale effect, can be interpreted by using this 'non-local', higher order theory. These effects are demonstrated for the cases of the unidirectional tension test, and for the small circular hole under uniform internal pressure commonly known as the inflation test. The latter configuration can be taken as a first order approximation of the indentation test that is frequently used for the laboratory or in situ characterization of geomaterials. In addition, it is shown that the solution of the three basic crack deformation modes leads to cusping of the crack tips that is caused by the action of 'cohesive' double forces behind and very close to the tips, that tend to bring the two opposite crack lips in close contact, and further, it is demonstrated that the fracture toughness depends on the size of the crack, and thus it is not a fundamental property of the material. This latter outcome agrees with experimental results which indicate that materials with smaller cracks are more resistant to fracture than those with larger cracks.

Keywords: Rock mechanics; Fracture mechanics Elasticity; Microstructure; Size effect; Brittle geomaterials

1. Introduction

Truesdell and Noll in the introduction of Non-Linear Field Theories of Mechanics (Encyclopedia of Physics, Vol. III/3, Sect. 3, 1965) state explicitly that:'… *Widespread is the misconception that those who formulate continuum theories believe matter 'really is' continuous, denying the existence of molecules. This is not so. Continuum physics presumes nothing regarding the structure of matter. It confines itself to relations among gross phenomena, neglecting the structure of the material on a smaller scale. Whether the continuum approach is justified, in any*

* Corresponding author. Tel: +30-821-37450; fax: +30-821-69554.

E-mail address: exadakty@mred.tuc.gr (G.E. Exadaktylos).

0040-1951/01/$ - see front matter
PII: S0040-1951(01)00047-6

particular case, is a matter, not for the philosophy or methodology of science, but for the experimental test…'. The theories of continuum mechanics use idealized models mostly based on the assumption of a continuous distribution of matter, as opposed to statistical theories of mechanics that are based on the assumption of a discrete distribution of matter. In our times this controversy still persists among those who believe that quantities which enter a continuum description should be seen as 'averages' of some other underlying 'microscopical' properties of the material, and those who do not accept this point of view. In the framework of continuum theories, quantities such as stress and strain, represent statistical mean values taken over very small ranges of volume. Consequently continuum theories cannot give satisfying predictions of the behavior of the material within very small ranges of volume, if high gradients of stress and strain occur. Especially, these theories cannot describe processes with dominating structure effects since all material qualities producing effects of such kind had been eliminated by introducing the idealized models. Within the field of strength of materials the above restriction becomes very important in connection with problems of high stress concentration as caused by extremely curved surfaces, e.g. at holes, notches and cracks. In such cases, the classical theory of elasticity predicts high values of stress and strain, which are replaced by mean values.

First, let us make a remark on the averaging procedure that is inherent in all continuum mechanics theories (e.g. Vardoulakis, 1997). Let us for simplicity consider an 1D case of a field, $y = f(x)$, whose mean value is computed over a small but finite averaging length L around a point x, that is

$$\langle y\rangle = \frac{1}{L}\int_{-L/2}^{L/2} f(x+\xi)\,\mathrm{d}\xi \tag{1}$$

If the field $f(x)$ varies linearly in the considered region around x, then it is approximated locally by a linear function, using an 1-term Taylor series expansion of the function f around point x, i.e.

$$f(x+\xi) \approx f(x) + f'(x)\xi \tag{2}$$

In the trivial case of a constant field then the first and all higher derivatives vanish and indeed the local value coincides with the average value. However, this is also true in case when the field varies locally linearly. Indeed we may then identify the field with its mean value over the considered averaging length, because by following the 'trapezoidal' integration rule, the value of a linearly varying field in the midpoint of the sampling interval is equal to its mean value in that interval

$$y = \langle y\rangle \tag{3}$$

that is to say, in this case the 'local' value y and the 'non-local' value $\langle y\rangle$ coincide. In a field theory where local values are identified with means according to rule (3) are called *simple theories* or *local theories* and the corresponding continua *locally homogeneous*. In case, however, where the considered field varies quadratically in the sampling region and a linear approximation is not sufficient, then we have to approximate it at least by a 2-term Taylor series expansion around point x

$$f(x+\xi) \approx f(x) + f'(x)\xi + \tfrac{1}{2}f''(x)\xi^2 \tag{4}$$

We notice that in the midpoint integration rule the effect of the first derivative is null. Thus for 'quadratically' varying fields, computational rule (3) must be enhanced, so as to incorporate the effect of the 'curvature'

$$y = \langle y\rangle - \frac{L^2}{24}\left.\frac{\mathrm{d}^2 y}{\mathrm{d}x^2}\right|_x + \mathrm{O}(L^4) \tag{5}$$

where the 'O' denotes the order-of-magnitude symbol. A general discussion of this issue may be also found in Muhlhaus et al. (1994). Field theories that are based on averaging rules that include the effect of higher gradients are called *higher gradient* or *nonlocal* theories. In particular, the above rule (5) represents a second gradient or grade-2 rule, and can be readily generalized in two and three dimensions by introducing the Laplacian operator instead of the second derivative in x.

The classical theory of elasticity requires that the forces between the atoms fulfil a very strong condition: the range of these forces must be small enough so that the stress (strain) measured at a point depends in the desired approximation only on the stress (strain) in the volume element around this point. Obviously, if interatomic forces did not reach farther than one atomic distance, a reaction against micro-deformation gradient would not exist and the theory does not have

an intrinsic length scale; this in turn leads to the undesirable result that a 10 cm slab behaves the same as a 10 μm film and there is no difference between a microcrack and a geological fault. However, since interatomic forces do, in principle, reach farther than one atomic distance a resistance against microdeformation gradient will be present, and therefore it is of no question whether gradient-dependent elasticity exists or not. The question is rather *how large* this effect may be.

The basic idea of taking into account not only the first but also the higher gradients of the displacement field in the expression for the strain energy function can be traced back to Bernoulli (1654–1705) and Euler (1707–1783) in connection with their work on beam theories. In elementary beam theory, with a section of the bar, there are associated two sets of kinematical quantities (a deformation vector and a rotation vector) and two sets of surface loads (tractions and bending couples). In plate theory, the situation is similar. The existence of surface and body couples independent of traction is fundamental to these theories. With the remarkable monograph of Cosserat and Cosserat (1909), this concept was extended to a 3D continuum where each point of the continuum is supplied with a set of mutually perpendicular rigid vectors (triad). The novel feature of their theory was the appearance of couple stresses in the equations of motion. An oriented continuum of this type was noted earlier by Voigt (1887) in connection with polar molecules in crystallography. Higher-order gradient and oriented media theories were rediscovered and/or reopened in various special forms and degree of complexity in the sixties. The state-of-the-art of this evolution in the mid-sixties was reflected in the collection of papers presented at the historical IUTAM Symposium on the "Mechanics of Generalized Continua", in Freudenstadt and Stuttgart in 1967 (Kröner, 1967). Newly, the interest to such theories is rekindled through the idea of connecting micromechanics with fracture and failure of solids (see for example Muhlhaus and Vardoulakis (1987), and for extensive literature review in Vardoulakis and Sulem (1995), chap. 8 and 9). The isotropic, higher-gradient, linear elasticity theory was developed essentially by Mindlin (1964, 1965). Mindlin's isotropic grade-3, linear elasticity theory with surface energy, which was further explored as far as its mathematical potential is concerned in a comprehensive paper by Wu (1992), includes 16 material constants plus the classical Lamé's constants. Since the presumption of material isotropy excludes the possibility to include a term linear in ε_{ijk} in the strain energy density expression w, where ε_{ijk} denotes the gradient of strain, Mindlin introduced in his theory self-equilibrating triple stresses in order to include surface free energy. This is clear if one considers that the strain gradient is a 3rd order tensor, and, in order to include its effect in w, one needs a director whose existence is excluded from the isotropy assumption. The surface free energy constant captures the desired surface phenomena in solids (Mindlin, 1965).

At the same time practically of publication of the pioneering papers by Mindlin, Professor Germain has encouraged the communication to the French Academy of Sciences of the ideas of Casal (1961, 1963, 1972), which in turn seem to have inspired Germain's (1973a,b) fundamental papers on the continuum mechanics structure of the grade-2 or higher grade theories. In our paper we want to give full credit to Casal's original idea, who was first to see the connection between surface tension effects and the anisotropic gradient elasticity theory. For this reason we provide here the simplest possible generalization of Casal's constitutive theory that accounts for only two material constants having the dimension of length: One, say ℓ, responsible for volumetric energy strain-gradient terms, and another, ℓ', responsible for surface energy strain-gradient terms. Casal considered the effect of the granular, polycrystalline and atomic nature of materials on their macroscopic response through the concept of internal and superficial capillarity expressed by the material lengths ℓ, ℓ', respectively, rather than through intractable statistical mechanics concepts. The concept that the surfaces of liquids are in a state of tension is a familiar one, and it is widely utilized. Actually it is known that no skin or thin foreign surface really is in existence at the surface, and that the interaction of surface molecules causes a condition analogous to a surface subjected to tension. The surface tension concept is therefore an analogy, but it explains the surface behavior in such satisfactory manner that the actual molecular phenomena need not be invoked. Of course such ideas are amenable to generalizations of various degrees of complexity. However, one should keep in

mind that already the determination of the two material lengths ℓ and ℓ' constitutes a formidable experimental challenge, and as it has been shown by Vardoulakis et al. (1998) and it will be shown here this might be possible only through carefully performed rock mechanics and rock fracture mechanics experiments.

The plan of the paper is as follows. In Section 2 the basic equations of anisotropic gradient elasticity theory with surface energy are reviewed. In Section 3 the problem of the infinite plate under normal tension is solved by taking into account of higher order strain gradients in the constitutive equations. Section 4 contains the presentation of displacement functions and complex variables. The analytical solution of the inflated circular hole problem is displayed in Section 5. Further, Section 6 is devoted to the investigation of strains and displacements in cracked solids.

2. Field equations and boundary conditions

2.1. Stress-equation of motion and boundary conditions

First it is noted that Casal's model cannot be directly embedded in Mindlin's (1964) linear, isotropic elasticity theory with microstructure because the former is an anisotropic elasticity model. Instead, Casal's expression for the global strain energy of the 1D tension bar was recovered by introducing an appropriate anisotropic, linear elastic, *restricted* Mindlin continuum. Mindlin's theory (Mindlin, 1964) introduced the idea of the 'unit cell' (micro-medium), which may be interpreted as the periodic structure of a crystal lattice, a crystal of a polycrystal, a grain of a granular rock, or the largest dimension of a constituent in the case of a heterogeneous rock mass. Appropriate kinematical quantities are then defined to describe geometrical changes in both the macro- and micro-medium. In case of a *restricted* Mindlin continuum the relative deformation γ_{ij} vanishes since the macroscopic strain coincides with the micro-deformation, i.e.

$$\gamma_{ij} = \partial_i u_j - \psi_{ij} \equiv 0 \tag{6}$$

In Eq. (6) u_i is the Cartesian component of the macro-displacement vector, ψ_{ij} denotes the micro-deformation (i.e. the displacement-gradient in the micro-medium) and $\partial_k \equiv \partial/\partial x_k$, with x_k to denote space coordinates $(k = 1, 2, 3)$. In this particular type of micro-homogeneous material the micro-deformation gradient (i.e. the macro-gradient of the micro-deformation) κ_{ijk} is identical with the gradient of strain, that is to say

$$\kappa_{ijk} = \kappa_{ikj} \equiv \partial_i \varepsilon_{jk} \tag{7}$$

in which

$$\varepsilon_{ij} \equiv \tfrac{1}{2}(\partial_j u_i + \partial_i u_j) \tag{8}$$

Next, the following *ansatz* for the potential energy density w (potential energy per unit macro-volume) is taken

$$w = w(\varepsilon_{ij}, \partial_k \varepsilon_{ij}) \tag{9}$$

Furthermore, since we are dealing with single-valued displacement fields one can easily establish a one-to-one correspondence between $\partial_k \varepsilon_{ij}$ and $\partial_k \partial_j u_i$ (Mindlin and Eshel, 1968). The variation of the total potential energy in volume V of the body is defined as follows (Mindlin, 1964, 1965)

$$\delta \int_V w \, \mathrm{d}V = \int_V (\tau_{ij} \delta \varepsilon_{ij} + \mu_{ijk} \partial_i \delta \varepsilon_{jk}) \, \mathrm{d}V \tag{10}$$

where

$$\tau_{ij} \equiv \frac{\partial w}{\partial \varepsilon_{ij}}, \qquad \mu_{ijk} \equiv \frac{\partial w}{\partial (\partial_i \varepsilon_{jk})} \tag{11}$$

The second order stress tensor τ_{ij}, which is dual in energy to the macroscopic strain, is symmetric, i.e. $\tau_{ij} = \tau_{ji}$ whereas the third order tensor μ_{ijk}, which is dual in energy to the strain-gradient, is called the double stress. The τ_{ij} are like the components of the usual stress with the dimensions of force per unit area, however, they depend on the second gradient of strain in addition to the strain. The 27 components μ_{kij} have the character of double forces per unit area. The first subscript of a double stress μ_{kij} designates the normal to the surface across which the component acts; the second and third subscripts have the same significance as the two subscripts of τ_{ij}. The eight components of the deviator of the couple-stress or couples per unit area formed by the combinations $(1/2)(\mu_{pqr} - \mu_{prq})$ are all equal to zero in the present gradient dependent elasticity theory, whereas all the remaining 10 independent combinations $(1/2)(\mu_{pqr} - \mu_{prq})$ are

self-equilibrating (Mindlin, 1964, 1965). Double force systems without moments are stress systems equivalent to two oppositely directed forces at the same point; such systems have direction but not net force and no resulting moment. Notice that singularities of this kind are discussed by Love (1927) and Eshelby (1951).

To prepare for the formulation of a variational principle, we apply the chain rule of differentiation and the divergence theorem; furthermore, we resolve $\partial_i u_j$ on the boundary ∂V of V into a plane-gradient and a normal-gradient as follows

$$\partial_i \delta u_j \equiv D_i \delta u_j + n_i D \delta u_j, \qquad D_i \equiv (\delta_{ik} - n_i n_k)\partial_k, \qquad D \equiv n_k \partial_k, \tag{12}$$

where δ_{ij} is the Kronecker delta and n_k is the outward unit normal on the boundary ∂V. The final expression for the variation in potential energy of a smooth boundary ∂V reads

$$\begin{aligned}\delta W = \int_V \delta w \, \mathrm{d}V = &- \int_V \partial_j(\tau_{jk} - \partial_i \mu_{ijk})\delta u_k \, \mathrm{d}V \\ &+ \int_{\partial V} n_j(\tau_{jk} - \partial_i \mu_{ijk})\delta u_k \, \mathrm{d}S \\ &+ \int_{\partial V} \left(\left[\frac{1}{R_1} + \frac{1}{R_2} \right] n_j - D_j \right) n_i \mu_{ijk} \delta u_k \, \mathrm{d}S \\ &+ \int_{\partial V} n_i n_j \mu_{ijk} D \delta u_k \, \mathrm{d}S \end{aligned} \tag{13}$$

where $(1/R_1 + 1/R_2)$ is the mean curvature of the bounding surface. Looking at the structure of Eq. (13) we now postulate the following form for the variation of work W_1 done by external forces

$$\delta W_1 = \int_V f_k \delta u_k \, \mathrm{d}V + \int_{\partial V} (\tilde{P}_k \delta u_k + \tilde{R}_k D \delta u_k) \, \mathrm{d}S \tag{14}$$

where f_k is the body force per unit volume, $\tilde{P}_k, \tilde{R}_k$ are the specified tractions and double tractions, respectively, on the smooth surface ∂V.

Next, we write Hamilton's principle for independent variations δu_i, $\partial_i \delta u_j$ between fixed limits of u_i and $\partial_i \delta u_j$ at times t_0 and t_1 (Love, 1927)

$$\delta \int_{t_0}^{t_1} (T - W) \, \mathrm{d}t + \int_{t_0}^{t_1} \delta W_1 \, \mathrm{d}t = 0 \tag{15}$$

where T is the total kinetic energy of the system. It can be shown that for the case of the restricted Mindlin continuum the following relationship is valid (Mindlin, 1964)

$$\begin{aligned}\delta \int_{t_0}^{t_1} T \, \mathrm{d}t = &- \int_{t_0}^{t_1} \mathrm{d}t \int_V \left[\rho \partial_{tt} u_k - \frac{1}{3} \rho d^2 \partial_i (\partial_{tt} \partial_i u_k) \right] \delta u_k \, \mathrm{d}V \\ &- \int_{t_0}^{t_1} \mathrm{d}t \int_{\partial V} \frac{1}{3} \rho d^2 n_i (D_i \partial_{tt} u_k + n_i D \partial_{tt} u_k) \delta u_k \, \mathrm{d}S \end{aligned} \tag{16}$$

wherein ρ is the mass of macro-material per unit macro-volume, d is the half-edge length of the cube of the micro-medium, and ∂_{tt} denotes double differentiation with respect to time. From relations (13)–(15) and (16) there follow the stress-equations of motion in the volume V

$$\partial_i \sigma_{ij} + f_j = \rho \partial_{tt} u_j - \frac{1}{3} \rho d^2 \partial_i (\partial_{tt} \partial_i u_j) \tag{17}$$

where we have set

$$\sigma_{ij} \equiv \tau_{ij} - \partial_k \mu_{kij} \tag{18}$$

We notice that according to Eq. (17) and for the static case the new stress tensor σ_{ij} is identified with the common macroscopic equilibrium stress tensor.

The surface ∂V of the considered volume V is divided into two complementary parts ∂V_u and ∂V_σ such that on ∂V_u kinematic data whereas on ∂V_σ static data are prescribed. In classical continua these are constraints on displacements and tractions, respectively. For the stresses the following set of six traction and double traction boundary conditions on a smooth surface ∂V_σ is also derived from the virtual work

principle (i.e. Eqs. (13), (14) and (16))

$$n_j\tau_{jk} - n_j\partial_i\mu_{ijk} + \left(\left[\frac{1}{R_1} + \frac{1}{R_2}\right]n_j - D_j\right)n_i\mu_{ijk} + \frac{1}{3}\rho d^2 n_j\left(D_j\partial_{tt}u_k + n_j D\partial_{tt}u_k\right) = \tilde{P}_k \tag{19}$$

$$n_i n_j \mu_{ijk} = \tilde{R}_k \tag{20}$$

Note that σ_{jk} given by Eq. (18) may be considered as the Cauchy stress tensor with the associated Cauchy stress vector t_k defined by

$$t_k \equiv n_j\sigma_{jk} = n_j\tau_{jk} - n_j\partial_i\mu_{ijk} \tag{21}$$

Since second-grade models introduce second strain gradients into the constitutive description, additional kinematic data must be prescribed on ∂V_u. With the displacement already given in∂V_u, only its normal derivative with respect to that boundary is unrestricted. This means that on ∂V_u the normal derivative of the displacement should also be given, i.e.

$$u_i = w_i \qquad \text{on } \partial V_{u1} \tag{22}$$

$$Du_i = r_i \qquad \text{on } \partial V_{u2} \tag{23}$$

2.2. Strain energy density function

The most general form of the strain energy density function for a linear, macroscopically homogeneous and isotropic, grade-2 elastic rock material is

$$\begin{aligned} w = {} & \frac{1}{2}\lambda\varepsilon_{ii}\varepsilon_{jj} + G\varepsilon_{ij}\varepsilon_{ji} + \mathcal{l}_{1k}\partial_k(\varepsilon_{ii}\varepsilon_{jj}) + \mathcal{l}_{2k}\partial_k(\varepsilon_{ij}\varepsilon_{ji}) \\ & + \mathcal{l}_{3j}\partial_k(\varepsilon_{ij}\varepsilon_{ik}) + \mathcal{l}_{4k}\partial_i(\varepsilon_{ij}\varepsilon_{kj}) + \mathcal{l}_{5k}\partial_j(\varepsilon_{ii}\varepsilon_{kj}) \\ & + a_1\partial_j\varepsilon_{ii}\partial_k\varepsilon_{ik} + a_2\partial_k\varepsilon_{ii}\partial_j\varepsilon_{kj} + a_3\partial_k\varepsilon_{ii}\partial_k\varepsilon_{jj} \\ & + a_5\partial_k\varepsilon_{ij}\partial_i\varepsilon_{kj} \end{aligned} \tag{24}$$

where λ and G are the usual Lamé constants, the five a_n are the additional constants which appear in Toupin's strain-gradient theory (Toupin, 1962; Mindlin, 1964), and $\mathcal{l}_{nk}$ ($n = 1,\ldots,5$; $k = 1,2,3$) are the five additional directors in order to include the effect of terms linear in the strain gradient, $\partial_i\varepsilon_{jk}$, in the strain energy density expression. The choice of the above polynomial expression for the strain energy density of the material with microstructure implies that terms of higher degree are small in comparison with those retained.

In Eq. (24) $\mathcal{l}_{nk}$ are characteristic directors such that

$$\mathcal{l}_{nk} \equiv \bar{\mathcal{l}}_n\nu_k,\ \nu_k\nu_k = 1; \qquad n = 1,\ldots,5,\ \ k = 1,2,3. \tag{25}$$

Accordingly Eq. (24) defines a gradient anisotropic elasticity with constant characteristic directors $\mathcal{l}_{nk}$. Also, the terms in Eq. (24) that are associated with these directors have the meaning of surface energy, since by using the divergence theorem one may find the following relations

$$\begin{aligned} &\int_V \partial_k(\mathcal{l}_{1k}\varepsilon_{ii}\varepsilon_{jj})\,\mathrm{d}V = \bar{\mathcal{l}}_1\int_{\partial V}(\varepsilon_{ii}\varepsilon_{jj})(\nu_k n_k)\,\mathrm{d}S, \\ &\int_V \partial_k(\mathcal{l}_{2k}\varepsilon_{ij}\varepsilon_{ji})\,\mathrm{d}V = \bar{\mathcal{l}}_2\int_{\partial V}(\varepsilon_{ij}\varepsilon_{ji})(\nu_k n_k)\,\mathrm{d}S, \\ &\int_V \partial_k(\mathcal{l}_{3j}\varepsilon_{ij}\varepsilon_{jk})\,\mathrm{d}V = \bar{\mathcal{l}}_3\int_{\partial V}(\varepsilon_{ij}\varepsilon_{ik})(\nu_j n_k)\,\mathrm{d}S, \\ &\int_V \partial_i(\mathcal{l}_{4k}\varepsilon_{ij}\varepsilon_{kj})\,\mathrm{d}V = \bar{\mathcal{l}}_4\int_{\partial V}(\varepsilon_{ij}\varepsilon_{kj})(\nu_k n_i)\,\mathrm{d}S, \\ &\int_V \partial_j(\mathcal{l}_{5k}\varepsilon_{ii}\varepsilon_{kj})\,\mathrm{d}V = \bar{\mathcal{l}}_5\int_{\partial V}(\varepsilon_{ii}\varepsilon_{kj})(\nu_k n_j)\,\mathrm{d}S. \end{aligned} \tag{26}$$

The ratios $\mathcal{l}_{nk}/G$ have the dimension of length whereas the ratios a_n/G have the dimension of square of length. The constitutive equations for the Cauchy and total stresses, as well as the double stresses are then derived by recourse to Eqs. (10), (11), (18) and (24) as it will be demonstrated in the next paragraphs.

3. An infinite plate under normal tension

For the special form of gradient elasticity that we consider here we assume that $\mathcal{l}_{2k} = G\mathcal{l}_k$ defined by Eq. (24) and $\alpha_4 = G\mathcal{l}^2$ are the only non-vanishing gradient coefficients, thus

$$w = \frac{1}{2}\lambda\varepsilon_{ii}\varepsilon_{jj} + G\varepsilon_{ij}\varepsilon_{ji} + G\mathcal{l}^2\partial_k\varepsilon_{ij}\partial_k\varepsilon_{ji} + G\mathcal{l}_k\partial_k(\varepsilon_{ij}\varepsilon_{ji}) \tag{27}$$

From relationships (10) and (11) and the above relation (27) follow the constitutive relations for the Cauchy stress and double stress tensors, respectively

$$\sigma_{ij} = \lambda\delta_{ij}\varepsilon_{kk} + 2G(\varepsilon_{ij} - \ell^2\nabla^2\varepsilon_{ij})$$
$$\mu_{kij} = 2G\ell_k\varepsilon_{ij} + 2G\ell^2\partial_k\varepsilon_{ij} \tag{28}$$

Let the Cartesian coordinates be $x_i (i = 1, 2, 3)$. Then consider the case of an infinite plate bounded by the surfaces $x_2 = \pm L$, subjected to uniform tension T perpendicular to those surfaces (Fig. 1). Accordingly in Eq. (28) $\ell_k = \ell'(k = 2)$ and $\ell_k = 0$ $(k \neq 2)$ is the material length scale associated with surface energy of the free surfaces $x_2 = \pm L$ of the plate. It is possible to assume, without loss of generality (e.g. it can be shown that, in this problem, the quantities u_1, u_3 do not couple with u_2 since these quantities satisfy homogeneous equations with homogeneous boundary conditions and therefore vanish identically), the following kinematical field

$$u_2(x_2) = u \tag{29}$$

Setting Eq. (29) into the first of relationships (28), employing the stress-equilibrium Eq. (17) for the static case, i.e. $\partial_{tt}u_j = 0$, and disregarding body forces, yields the field equation

$$u^{\mathrm{IV}} - \frac{a+2}{2\ell^2}u'' = 0; \qquad a = \frac{\lambda}{G} \tag{30}$$

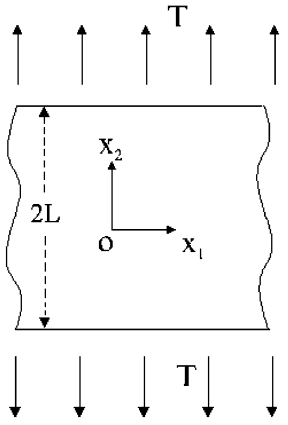

Fig. 1. Infinite plate bounded by surfaces at distance L apart under uniform uniaxial tension, and coordinates.

The general solution of Eq. (30) is the following

$$u = c_1 + c_2x + c_3e^{a'x/\ell} + c_4e^{-a'x/\ell};$$
$$a' = \sqrt{\frac{a+2}{2}} = \sqrt{\frac{1-\nu}{1-2\nu}} \tag{31}$$

where we have set $x_2 = x$, and $c_i\,(i = 1, \ldots, 4)$ are unknown constants to be determined from the following boundary conditions (20) and (21) which are valid at $x_2 = \pm L$

$$\sigma_{22} = 2G(a'^2u' - \ell^{-2}u''') = T, \qquad \sigma_{21} = 0,$$
$$\mu_{222} = 2G(\mathrm{sgn}(x)\ell'u' + \ell^2u'') = 0, \mu_{221} = 0 \tag{32}$$

where the symbol $\mathrm{sgn}(\cdot)$ denotes the signum function. It may be noted that for $c_3 = c_4 = 0$ the deformation is homogeneous and is referred as a 1st gradient continuum theory. Substituting in Eq. (32) the expression for the displacement in the frame of the present 2nd gradient theory given in Eq. (31) we finally obtain

$$c_1 = 0, \qquad c_2 = \frac{T}{2Ga'^2},$$
$$c_3 = -c_4 = -\frac{\ell'T}{4Ga'^3\left(\frac{\ell'}{\ell}\sinh a'\bar{L} + a'\cosh a'\bar{L}\right)} \tag{33}$$

in which $\bar{L} = L/\ell$. The strain of the plate $\varepsilon_{22} = \varepsilon$ can be found to be

$$\varepsilon(\bar{x}) = \frac{T}{(\lambda + 2G)}\left\{1 - \frac{k\cosh a'\bar{x}}{(k\sinh a'\bar{L} + a'\cosh a'\bar{L})}\right\},$$
$$k = \frac{\ell'}{\ell} \tag{34}$$

with $\bar{x} = x/\ell$.

The distribution of the normalized strain $\varepsilon/T/(\lambda + 2G)$ along the height $-\bar{L} \leq \bar{x} \leq \bar{L}$ of the tension-specimen is displayed in Fig. 2. It is shown that the strain distribution corresponding to *homogeneous* tension is not anymore homogeneous, and depending on the sign of the relative *surface energy parameter k* reaches its maximum $(k > 0)$ or minimum $(k < 0)$ value, respectively, at the mid-height of the specimen. Hence, experimental observations that macroscopically uniform material domains, under uniform

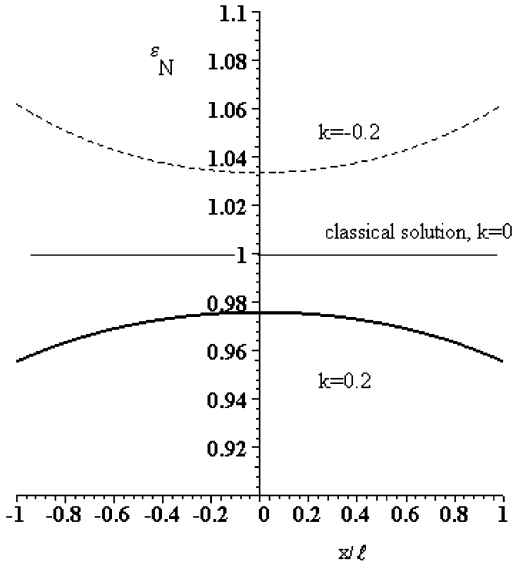

Fig. 2. Normalized strain distribution $\varepsilon/T/(\lambda + 2G)$ along the height of the specimen ($\bar{L} = L/\ell = 1$) for two values of the relative surface energy parameter and for Poisson's ratio $\nu = 1/4$.

surface tractions develop localized, i.e. non-uniform deformation fields in contrast to 'local' theories, are predicted by the present grade-2 theory. This property of the solution is a clear indication that the gradient elasticity with $k > 0$ can be employed as a potential model to explain the *necking phenomenon* or the strain localization in rocks. On the other hand, for negative value of k the gradient strain localizes at the edges of the specimen and attains a higher value than that predicted by the classical elasticity theory. Finally, for $k = 0$, the gradient elasticity solution (34) degenerates into the classical elasticity solution. These properties may also be used to establish the surface gradient parameter k through carefully performed uniaxial tension experiments.

By defining an extensional failure criterion of the *Saint-Venant* type, i.e. $\varepsilon = \varepsilon_c$ at $x = 0$ for the necking type of specimen failure (e.g. $k < 0$) and a strain concentration factor, as usually, by the ratio $\varepsilon/T/(\lambda + 2G)$ at $x = 0$, we can obtain the behavior depicted in Fig. 3 for the variation of the normalized failure strain $\hat{\varepsilon} = T/(\lambda + 2G)/\varepsilon_c$ with the dimensionless semi-height $\bar{L} = L/\ell$ and the relative surface energy ratio k of the tension specimen. The behavior depicted in Fig. 3 is consistent with rock mechanics experimental observations which show that smaller specimens fail at higher stress than larger specimens.

For the special 1D case considered above the strain energy density expression (27) can be written in the form

$$w/(\lambda + 2G) = (\varepsilon \quad \varepsilon') \begin{pmatrix} a' & k \\ k & 1 \end{pmatrix} \begin{pmatrix} \varepsilon \\ \varepsilon' \end{pmatrix} \tag{35}$$

The quadratic form (35) is positive definite — implying that energy is stored, rather than produced — if the eigenvalues of the square matrix are all positive (Pettofrezzo, 1978). It can be easily verified that the eigenvalues are the following

$$\lambda_{1,2} = \frac{(1 + a'^2) \pm \sqrt{(1 - a'^2)^2 + 4k^2}}{2} \tag{36}$$

and are always positive if the following inequality holds true

$$-\sqrt{\frac{1 - \nu}{1 - 2\nu}} < k < \sqrt{\frac{1 - \nu}{1 - 2\nu}}. \tag{37}$$

Provided that inequalities (37) are valid the uniqueness of the problem at hand defined by displacement-equilibrium Eq. (30) and boundary conditions (32) is also proven.

4. Displacement functions

For the special form of gradient elasticity that we consider here we assume that ℓ_{1k}, ℓ_{2k}, a_3, and a_4 are the only non-vanishing gradient coefficients. Thus, by setting into Eq. (24)

$$\ell_{1k} = \frac{\lambda}{2}\ell_k, \qquad \ell_{2k} = G\ell_k, \qquad a_3 = \frac{\lambda}{2}\ell^2, \qquad a_4 = G\ell^2 \tag{38}$$

with ℓ_k defined by Eq. (25), we find the following expression for the strain energy density function for a macroscopically homogeneous and isotropic

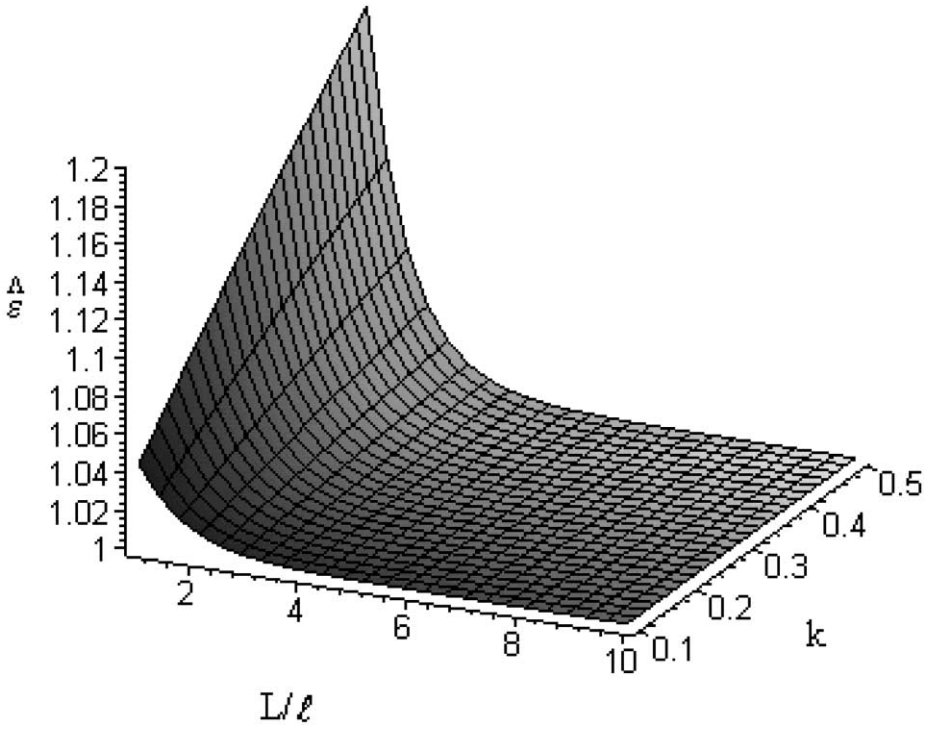

Fig. 3. Dependence of the normalized failure strain on specimen's size (size effect) for various positive values of the surface energy parameter and for Poisson's ratio $\nu = 1/4$.

geomaterial

$$\begin{aligned} \mathrm{w} = {} & \frac{1}{2}\lambda\varepsilon_{ii}\varepsilon_{jj} + G\varepsilon_{ij}\varepsilon_{ji} + \frac{1}{2}\lambda\ell^2\partial_k\varepsilon_{ii}\partial_k\varepsilon_{jj} \\ & + G\ell^2\partial_k\varepsilon_{ij}\partial_k\varepsilon_{ji} + \frac{1}{2}\lambda\ell_k\partial_k\Big(\varepsilon_{ii}\varepsilon_{jj}\Big) \\ & + G\ell_k\partial_k\Big(\varepsilon_{ij}\varepsilon_{ji}\Big) \qquad i,j,k = 1,2,3 \end{aligned} \tag{39}$$

From the above definition (39) as well as definitions (10) and (11) follow the constitutive relations for the Cauchy stress and double stress tensors, respectively

$$\sigma_{ij} = \Big(1 - \ell^2\nabla^2\Big)\Big(\lambda\delta_{ij}\varepsilon_{kk} + 2G\varepsilon_{ij}\Big) \tag{40}$$

$$\mu_{kij} = \ell_k\Big(\lambda\delta_{ij}\varepsilon_{\ell\ell} + 2G\varepsilon_{ij}\Big) + \ell^2\partial_k\Big(\lambda\delta_{ij}\varepsilon_{\ell\ell} + 2G\varepsilon_{ij}\Big)$$

Note that the above definition of Cauchy stress may be derived by assuming that Hooke's law is generalized through averaging of σ_{ij} in a Representative Elementary Volume (REV) of the material, i.e.

$$\langle\sigma_{ij}\rangle = \int_{\mathrm{REV}} \sigma_{ij}\,\mathrm{d}V = \lambda\delta_{ij}\varepsilon_{kk} + 2G\varepsilon_{ij} \tag{40a}$$

Then according to relationship (5) the above assumption leads to the first of constitutive Eq. (40). Substituting in stress equilibrium Eqs. (17) (for $\partial_{tt}u_j = 0$) the constitutive relation for the total stress given by the first of Eq. (40) and expressing the strains in terms of displacements through Eq. (8), we obtain the following displacement equation of equilibrium in vector notation

$$G\bar{D}^2\{\bar{m}\nabla\nabla\cdot\underset{\sim}{u} + \nabla^2\underset{\sim}{u}\} + \underset{\sim}{f} = 0; \quad \bar{m} = \frac{\lambda + G}{G} \tag{41}$$

where the curly underline of a symbol means that this is a vector, ∇ is the gradient operator, ∇ is the divergence operator, and the operator $\bar{D}^2$ is defined as follows

$$\bar{D}^2 \equiv 1 - \ell^2\nabla^2 \tag{42}$$

As it is observed from the above Eq. (41) the constant $\mathcal{L}'$, even when properly included in the constitutive equations, does not appear in the displacement equations of equilibrium. Nevertheless, it may enter the displacement field through certain of the boundary conditions. It is also important to observe that in the limit $\mathcal{L} \to 0$ the highest derivative term in Eq. (42) is lost, suggesting the emergence of boundary layer effects at bimaterial interfaces. It may be proved that any solution $\underset{\sim}{u}$ of the displacement-equation of equilibrium (41) can be expressed as

$$\underset{\sim}{u} = \underset{\sim}{B} - \mathcal{L}^2 \nabla\nabla\cdot\underset{\sim}{B} - \frac{1}{2}\nabla\left(\bar{D}^2 - \frac{1}{\tilde{m}}\right)\left[\underset{\sim}{r}\cdot\bar{D}^2\underset{\sim}{B} + B_0\right], \tag{43}$$

$$G\nabla^2\bar{D}^2 B_0 = \underset{\sim}{r}\cdot\bar{D}^2\underset{\sim}{f} - 4\mathcal{L}^2\nabla\cdot\underset{\sim}{f}, \qquad G\nabla^2\bar{D}^2\underset{\sim}{B} = -\underset{\sim}{f}$$

wherein

$$\tilde{m} = \frac{\lambda + 2G}{G}$$

It is worth noting that the functions $\underset{\sim}{B}$, B_0 reduce to *Neuber's–Papkovich's* functions when $\mathcal{L} = 0$. A further simplification of the displacement representation (43) results by noting that the stress field predicted by the present gradient theory remains the same as that obtained from the classical solution of a corresponding boundary value problem with imposed traction (Ru and Aifantis, 1993). Hence, in static plane strain conditions the displacements can be expressed in tensorial form as follows

$$2Gu_i = 4(1-\nu)B_i - (x_j B_j + B_0)_{,i} - 2l^2 B_{j,ji} + u_i^+; \quad i,j = x,y. \tag{44}$$

in which $B_i (i = x, y)$ and B_0, are identified with the classical displacement harmonic functions, and u_x^+, u_y^+ are extra functions that are associated with the higher order strain gradients and obey the Helmholtz's equation

$$\bar{D}^2 u_i^+ = 0; \qquad i = x, y \tag{45}$$

It is possible to take one of B_x, B_y equal to zero (e.g. Sternberg and Gurtin (1962)), but a more elegant theory may be derived by virtue of the complex function theory which has been developed in a rigorous manner by Muskhelishvili (1963). It may be shown that the following complex representation for the displacements holds true

$$2G(u + \mathrm{i}v) = \kappa\phi_c(z) - \bar{\psi}_c(\bar{z}) - z\overline{\phi_c'(z)} - 4\mathcal{L}^2\bar{\phi}_c''(\bar{z}) + (u^+ + \mathrm{i}v^+) \tag{46}$$

where we have used the identities $\partial/\partial z \equiv (1/2)\times(\partial/\partial x - \mathrm{i}\partial/\partial y)$, and $\partial/\partial\bar{z} \equiv (1/2)(\partial/\partial x + \mathrm{i}\partial/\partial y)$, with $\bar{z} = x - \mathrm{i}y$ to be the complex conjugate of $z = x + \mathrm{i}y$, the prime denotes differentiation with respect to z, and $i \equiv \sqrt{-1}$ is the usual imaginary unit. Also, in relation (46) we have set $u = u_x$, $v = u_y$, $u^+ = u_x^+$, $v^+ = u_y^+$ whereas $\phi_c(z)$, $\psi_c(z)$ are analytical complex functions and $\kappa = 3 - 4\nu$ or $\kappa = (3-\nu)/(1+\nu)$ is *Muskhelishvili's* constant for plane strain or generalized plane stress conditions, respectively. It may be observed that for $\mathcal{L} = 0$, relationship (48) reduces to the *Kolosov-Muskhelishvili* solution (Muskhelishvili, 1963, p.112).

Then, the strains, and stresses referred to the Cartesian coordinates x, y can be found as follows

$$2G(\varepsilon_{xx} + \varepsilon_{yy}) = (\kappa - 1)\{\phi_c'(z) + \bar{\phi}_c'(\bar{z})\} + (u_{,x}^+ + v_{,y}^+),$$

$$2G(\varepsilon_{yy} - \varepsilon_{xx} + 2i\varepsilon_{xy}) = 2\left\{\psi_c'(z) + \bar{z}\phi_c''(z) + 4\mathcal{L}^2\phi_c'''(z) - \frac{\partial}{\partial z}(u^+ - iv^+)\right\},$$

$$\sigma_{xx} + \sigma_{yy} = 2[\phi_c'(z) + \overline{\phi_c'(z)}],$$

$$\sigma_{yy} - \sigma_{xx} + 2i\sigma_{xy} = 2[\bar{z}\phi_c''(z) + \psi_c'(z)]. \tag{47}$$

The following complex representation can be also found for the double stresses μ_{yyy}, μ_{yyx}

$$\mu_{yyy} + \mathrm{i}\mu_{yyx} = (\mathcal{L}' + \mathcal{L}^2\partial_y) \times\left\{\frac{\kappa - 1}{2(1-2\nu)}\left[\phi_c'(z) + \overline{\phi_c'(z)}\right] + \left[\psi_c'(z) + \bar{z}\phi_c''(z) + 4\mathcal{L}^2\phi_c'''(z)\right] + \frac{1}{2(1-2\nu)}(u_{,x}^+ + v_{,y}^+) - \frac{\partial}{\partial z}(u^+ - iv^+)\right\} \tag{48}$$

Denote further by u_r, u_θ and ε_{rr}, $\varepsilon_{\theta\theta}$, $\varepsilon_{r\theta}$, respectively, the displacement and strain components referred to the polar coordinates r, θ with origin exactly at the origin of the Cartesian coordinate system. There are the following representation formulae

$$2G(u_r + \mathrm{i}u_\theta) = \mathrm{e}^{-\mathrm{i}\theta}\{\kappa\phi_c(z) - \bar{\psi}_c(\bar{z}) - z\overline{\phi_c'(z)} - 4\ell^2\bar{\phi}_c''(\bar{z}) + (u^+ + iv^+)\},$$

$$2G(\varepsilon_{rr} + \varepsilon_{\theta\theta}) = (\kappa - 1)\{\phi_c'(z) + \overline{\phi_c'(z)}\} + (u_{,x}^+ + v_{,y}^+),$$

$$2G(\varepsilon_{\theta\theta} - \varepsilon_{rr} + 2\mathrm{i}\varepsilon_{r\theta}) = 2\mathrm{e}^{2\mathrm{i}\theta}\Big\{\psi_c'(z) + \bar{z}\phi_c''(z) + 4\ell^2\phi_c'''(z) - \frac{\partial}{\partial z}(u^+ - \mathrm{i}v^+)\Big\},$$

$$\sigma_{rr} + \sigma_{\theta\theta} = 2\Big[\phi_c'(z) + \overline{\phi_c'(z)}\Big],$$

$$\sigma_{\theta\theta} - \sigma_{rr} + 2i\sigma_{r\theta} = 2e^{2i\theta}\Big\{\bar{z}\phi_c''(z) + \psi_c'(z)\Big\},$$

$$\mu_{rrr-i\mu rr\theta} = \mathscr{L}' + \mathscr{L}^2\partial_r\Big\{\frac{\kappa-1}{2(1-2\nu)}\Big[\phi_c'(z) + \overline{\phi_c'(z)}\Big] - \mathrm{e}^{2\mathrm{i}\theta}[\psi_c'(z) + \bar{z}\phi_c''(z) + 4\ell^2\phi_c'''(z)] + \frac{1}{2(1-2\nu)}(u_{,x}^+ + v_{,y}^+) + \mathrm{e}^{2\mathrm{i}\theta}\frac{\partial}{\partial z}(u^+ - \mathrm{i}v^+)\Big\}$$

5. Circular hole subjected to all-around pressure in an infinite plane

5.1. Solution

In a first attempt the problem of all-around pressurized circular hole is considered. The elastic solution of the inflated circular hole (or cavity-expansion) is of considerable practical interest in the investigation of surface-removal processes on elastic–brittle rocks, rock mass characterization by recourse to indentation-type operations, borehole stability problems and other. It is noted here that the stress-strain field produced by a cavity-expansion is recovered as the leading-order approximation of the rigid, slender indenter (Norbury and Wheeler, 1987).

For this purpose let us consider the case when the edge of a long circular hole is subject to uniform normal pressure P, the double tractions vanish at the hole boundary, and the stresses and double stresses vanish at infinity. The traction boundary conditions according to Eqs. (20) and (21) take the form

$$\sigma_{rr} - \mathrm{i}\sigma_{r\theta} = -P,\ \mu_{rrr} - \mathrm{i}\mu_{rr\theta} = 0 \ \text{ at } \ r = R \tag{50}$$

whereas the following regularity conditions at infinity are valid

$$\sigma_{ij} \to 0, \qquad \mu_{ijk} \to 0 \quad (i,j,k = r,\theta) \text{ as } r = \sqrt{x^2 + y^2} \to \infty \tag{51}$$

The solution of the problem at hand which satisfies the equilibrium equations and the first of conditions (50) in the form of complex potentials is given by Muskhelishvili (1963) as follows

$$\phi_c(z) = 0, \qquad \psi_c(z) = -\frac{PR^2}{z} \tag{52}$$

where $z = re^{\mathrm{i}\theta}$. Furthermore, the following representations of the extra gradient functions that satisfy Eq. (45) are valid in the region outside the contour of the hole

$$u^+(x,y) = \sum_{-\infty}^{\infty}\beta_k K_k(\lambda r)\,\mathrm{e}^{\mathrm{i}k\theta}, \qquad v^+(x,y) = \sum_{-\infty}^{\infty} c_k K_k(\lambda r)\,\mathrm{e}^{\mathrm{i}k\theta} \tag{53}$$

$$\lambda = \ell^{-1}, \beta_{-k} = \bar{\beta}_k, c_{-k} = \bar{c}_k$$

where $K_n(\cdot)$ is the Bessel function of the second kind of the imaginary argument and nth order (Macdonald's function). By using the differentiation rule for the function K_n (see for example Watson (1966)), we obtain

$$\frac{\partial u^+(x,y)}{\partial z} = -\frac{1}{2}\sum_{-\infty}^{\infty}\lambda\beta_{k+1}K_k(\lambda r)\,\mathrm{e}^{\mathrm{i}k\theta}, \qquad \frac{\partial u^+(x,y)}{\partial \bar{z}} = -\frac{1}{2}\sum_{-\infty}^{\infty}\lambda\beta_{k-1}K_k(\lambda r)\,\mathrm{e}^{\mathrm{i}k\theta} \tag{54}$$

Under these circumstances by substituting Eqs. (52)–(54) into the second of conditions (50), setting $z = \mathrm{Re}^{\mathrm{i}\theta}$, equating the result with zero, and comparing

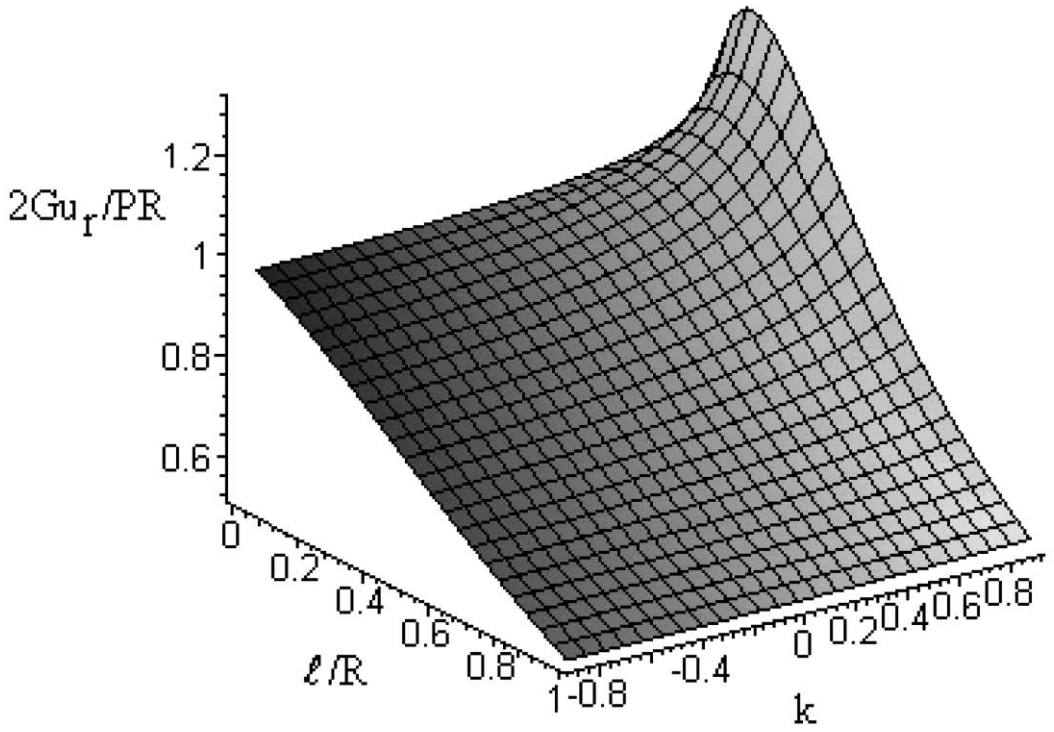

Fig. 4. Plot of the dependence of the dimensionless radial displacement on the relative volume energy length scale ℓ/R and on the ratio of surface length over the volume length, k for Poisson's ratio $\nu = 0.25$.

coefficients of $e^{ik\theta}$ one finds

$$k = 0 : (\beta_1 + ic_1)A_0(R) + 2(1-2\nu)(\bar{\beta}_1 - i\bar{c}_1)B_0(R)$$

$$= 4(1-2\nu)P\ell\left(\ell' - \frac{2\ell^2}{R}\right),$$

$$k \geq 1 : (\beta_{k+1} + ic_{k+1})$$

$$\times (A_k)(R) + 2(1-2\nu)(\beta_{k-1} - ic_{k-1})B_k(R)$$

$$= 0, 2(1-2\nu)(\beta_{k+1} + ic_{k+1})B_{-k}(R)$$

$$+ (\beta_{k-1} - ic_{k-1})A_{-k}(R) = 0. \tag{55}$$

in which

$$A_k(r) = -(\ell' + \ell^2\partial_r)K_k(\lambda r),$$

$$B_k(r) = -(\ell' + \ell^2\partial_r)\left[\frac{1}{2(1-2\nu)}K_k(\lambda r) + K_{k-2}(\lambda r)\right]. \tag{56}$$

The differentiations in Eq. (56) may be facilitated by the identities (Watson, 1966)

$$\frac{\partial K_n(\lambda' r)}{\partial r} = -\frac{n}{r}K_n(\lambda' r) - \lambda' K_{n-1}(\lambda' r), K_{-n} = K_n. \tag{56a}$$

It may be shown from Eq. (55) that the following equations are valid

$$\mathrm{Re}(\beta_1) = \left[(1-2\nu)P\left(k - \frac{2}{\lambda R}\right)\right] \Big/$$

$$\left[2\lambda\left\{\left[\frac{(1-2\nu)}{\lambda R} - (1-\nu)k\right]K_0(\lambda R)\right.\right.$$

$$\left.\left. + \left[(1-\nu) + \frac{(1-2\nu)}{\lambda R}\left(\frac{2}{\lambda R} - k\right)\right]K_1(\lambda R)\right\}\right],$$

$$\mathrm{Im}(c_1) = -\mathrm{Re}(\beta_1), \mathrm{Im}(\beta_1) = \mathrm{Re}(c_1) = 0,$$

$$\beta_0 = c_0 = 0, \quad \beta_{\pm n} = c_{\pm n} = 0 \quad (n \geq 2) \tag{57}$$

where Re(·) and Im(·) denote the real and imaginary value of what they enclose, respectively. In view of Eqs. (53) and (57) the extra gradient displacement field can be found to be

$$u^+ + \mathrm{i}v^+ = 2\mathrm{Re}(\beta_1)K_1(\lambda r)\,\mathrm{e}^{\mathrm{i}\theta} \tag{58}$$

By virtue of the first of Eqs. (49), (52), (57) and (58) we finally obtain the displacement and strain fields around the hole as follows

$$2Gu_r = \frac{PR^2}{r} + \left[P(1-2\nu)\left(k - \frac{2}{\lambda R}\right)K_1(\lambda r)\right] \Bigg/ \left[\lambda\left\{\left[\frac{(1-2\nu)}{\lambda R} - (1-\nu)k\right]K_0(\lambda R) + \left[(1-\nu) + \frac{(1-2\nu)}{\lambda R}\left(\frac{2}{\lambda R} - k\right)\right]K_1(\lambda R)\right\}\right],$$

$$u_\theta = 0,$$

$$2G\varepsilon_{\theta\theta} = \frac{PR^2}{r^2} + \left[P(1-2\nu)\left(k - \frac{2}{\lambda R}\right)K_1(\lambda r)\right] \Bigg/ \left[(\lambda r)\left\{\left[\frac{(1-2\nu)}{\lambda R} - (1-\nu)k\right]K_0(\lambda R) + \left[(1-\nu) + \frac{(1-2\nu)}{\lambda R}\left(\frac{2}{\lambda R} - k\right)\right]K_1(\lambda R)\right\}\right],$$

$$2G\varepsilon_{rr} = -\frac{PR^2}{r^2} - \left[P(1-2\nu)\left(k - \frac{2}{\lambda R}\right)[(\lambda r)K_0(\lambda r) + K_1(\lambda r)]\right] \Bigg/ \left[(\lambda r)\left\{\left[\frac{(1-2\nu)}{\lambda R} - (1-\nu)k\right]K_0(\lambda R) + \left[(1-\nu) + \frac{(1-2\nu)}{\lambda R}\left(\frac{2}{\lambda R} - k\right)\right]K_1(\lambda R)\right\}\right],$$

$$\varepsilon_{r\theta} = 0, \tag{59}$$

where we have set the non-dimensional surface energy variable $k = (\ell')/\ell$. Finally, it may be demonstrated that the stress field remains the same with that predicted by classical elasticity, i.e.

$$\sigma_{rr} = -\frac{PR^2}{r^2}, \qquad \sigma_{\theta\theta} = \frac{PR^2}{r^2}, \qquad \sigma_{r\theta} = 0. \tag{60a}$$

The asymptotic expansions of the radial displacement for the volumetric strain gradient parameter tending to zero and to infinity may be also derived

$$2Gu_r|_{\ell\to 0} \cong R + o(\ell), \qquad 2Gu_r|_{\ell\to\infty} \cong o(\ell^{-2}) \tag{60b}$$

Fig. 4 presents the 3D plot of the dimensionless radial displacement at hole wall vs. the relative volume energy length scale and the relative surface energy term for a given Poisson's ratio of the material. It is observed that:

1. For a given value of R and k the radial displacement decreases as the volume length scale increases. This result may be also interpreted by saying that the radial displacement of the hole wall increases as the radius of the hole increases for given characteristic length of the rock microstructure ℓ. This result is in accordance with experimental evidence, namely that the convergence of the wall of a deep borehole in a compressive field increases as its radius increases.
2. For a given value of R and volume length scale ℓ/R the radial displacement increases as the surface energy length scale increases.

Also Fig. 5 shows the dependence of the dimensionless radial displacement at hole wall vs. the relative volume energy length scale ℓ/R and the Poisson's ratio of the material for a zero relative surface energy term. It may be seen that the uniformly pressurized hole becomes stiffer as Poisson's ratio of the rock decreases with this effect to be more pronounced for large values of ℓ/R.

5.2. Size effect and pressure–strain relation in indentation tests

A notorious feature of brittle amorphous or crystalline materials such as glass, ceramics, rocks, concretes and other, is their tendency to become stronger as the area under stress is decreased. Herein we consider the maximum extension strain failure hypothesis

proposed by Poncelet (1788–1867) and referred by the famous *Barré de Saint-Venant* in his notes 'Historique abrégé des Recherches sur la résistance et sur l'(lasticité des corps solides', pp. xc–cccxi in his annotated third edition (Paris, 1864) of the section 'De la résistance des corps solides' of Navier's '*Résumé des leçons donéesà l'(cole des Ponts et Chaussées sur l'application de la mécaniqueà l'(tablissement des constructions et des machines*' which maybe stated as: ' *Fracture of a brittle material will initiate when the total extension strain in the material exceeds a critical value which is characteristic of that material*'. It is worth noting that Stacey (1981) has applied successfully the above limiting extension strain criterion to the prediction of fracture in brittle rocks, although no explicit reference to *Saint-Venant's* original work is made. For the internally pressurized circular hole the maximum extension strain criterion takes the form

$$\varepsilon_{\theta\theta} = \varepsilon_c \text{ at } >,\ r = R \tag{61}$$

where $\varepsilon_{\theta\theta}$ is the tangential strain or hoop strain, and ε_c is the critical value of extension strain which is intrinsic property of the material. Then, following the same procedure as in the previous paragraph for the tension specimen, we define a strain concentration factor by the ratio $\varepsilon_{\theta\theta}/(P/2G)$ at $r = R$, so that from the third of Eq. (58) we obtain the normalized failure strain ε_{ef}

$$\varepsilon_{ef} = \frac{1}{\{1 - \hat{\varepsilon}\}} \tag{62}$$

where

$$\varepsilon_{ef} = \frac{1}{\varepsilon_c/(P/2G)} = \frac{1}{\varepsilon_{\theta\theta}/(P/2G)} \qquad \text{at failure} \tag{63}$$

and

$$\hat{\varepsilon} = \left[(1-2\nu)\left(k - \frac{2}{\lambda R}\right)K_1(\lambda R)\right] \Bigg/ \left[(\lambda R)\left\{\left[\frac{(1-2\nu)}{\lambda R} - (1-\nu)k\right]K_0(\lambda R) + \left[(1-\nu) + \frac{(1-2\nu)}{\lambda R}\left(\frac{2}{\lambda R} - k\right)\right]K_1(\lambda R)\right\}\right] \tag{63a}$$

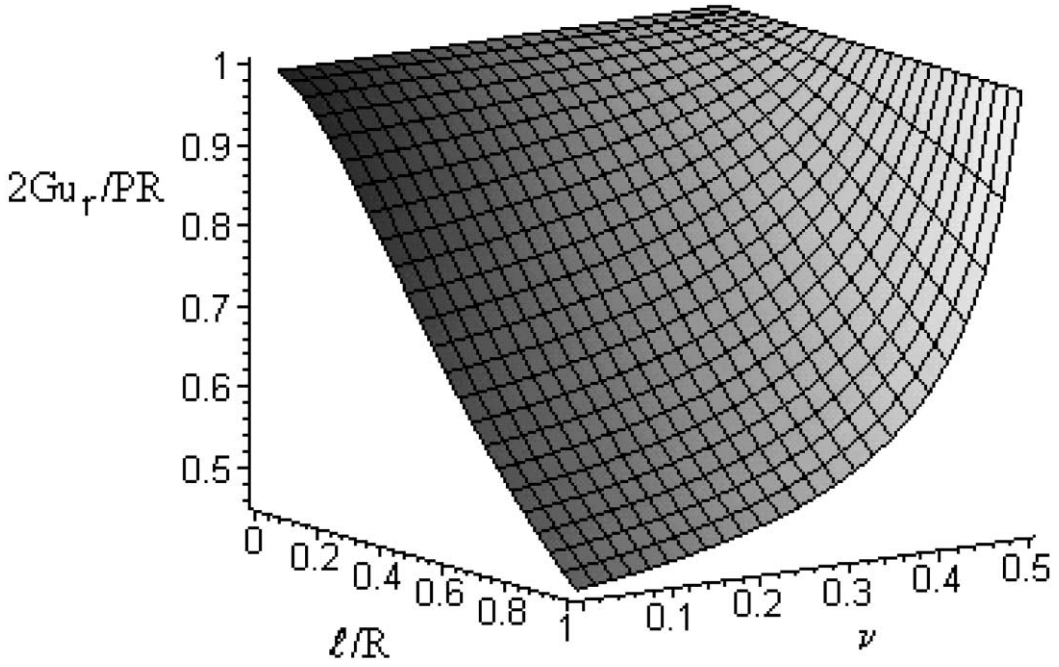

Fig. 5. Plot of the dependence of the dimensionless radial displacement on the relative volume energy length scale, ℓ/R, and on Poisson's ratio for $k = 0$.

By using the asymptotic formula

$$K_n(x) = \frac{2^{n-1}(n-1)!}{x^n} + o(x^{-n}) \tag{63b}$$

suitable for small x and after some elaboration, we pass from Eq. (62) to the following inner approximation or boundary layer solution for the normalized failure strain for small $\hat{R}$

$$\varepsilon_{\mathrm{ef}} = \frac{2(1-2\nu)}{C}\hat{R}^{-2} + k\frac{(1-2\nu)[\log(2\hat{R}^{-1}) - \gamma - (1-\nu)]}{C^2}\hat{R}^{-1} + O(1) \quad (\text{small } \hat{R}) \tag{64}$$

wherein

$$C = (1-2\nu)\{\log(2\hat{R}^{-1}) - \gamma\} + 1 - \nu \tag{64b}$$

and $\gamma = 0.5772156649\ldots$ is Euler's constant. On the other hand, for sufficiently large $\hat{R}$ the outer approximation is

$$\varepsilon_{\mathrm{ef}} = 1 + O(\hat{R}^{-1}) \quad (\text{large } \hat{R}) \tag{65}$$

For the intermediate values of $\hat{R}$ we can get a closed form expression of $\varepsilon_{\mathrm{ef}}$ by using the exact solution (62). Eq. (64) indicates that there is a size effect, which is understood as the dependence of nominal strain at failure (nominal strength, in our case expressed by $\varepsilon_{\mathrm{ef}}$) on the size-in our case the normalized hole radius R/ℓ, provided that geometrically similar situations are compared. It should be noted that in the theory of linear elasticity and in any theory of conventional plasticity there is no size effect (e.g. in Bazant and Cedolin 1991, chap. 12 and 13).

Fig. 6 displays the dependence of the normalized failure strain ε_{ef} on the dimensionless radius of the pressurized hole R/ℓ for various values of the relative surface energy strain-gradient parameter $k = \ell'/\ell$ according to the formulae (59) and (62). As is apparent, the normalized failure strain decreases monotonically in the departure from the gradient-dependent elasticity theory, i.e. as R increases with respect to the volume energy strain-gradient parameter ℓ, and tends asymptotically to the value of 1 that is predicted by the classical theory. In Fig. 6 it is also demonstrated that the relative surface energy parameter k expresses the intensity of the size effect. As it is shown, the effect of negative surface energy term is to increase the maximum extensional strain sustained by the hole (stiffer hole), whereas the effect of positive surface energy term is to decrease the maximum strain, or alternatively, to increase the compliance of the hole. It is also seen that for sufficiently large k and R/ℓ the value of the failure strain is slightly lower than the classical value; however, the asymptotic value of the normalized failure strain of the inflated hole in the limit as $R/\ell \to \infty$ for every k, ν is given by the formula

$$\lim_{R/\ell\to\infty} \varepsilon_{\mathrm{ef}} = 1 \tag{65b}$$

The consistency of the size effect predicted herein can be checked with Tillet's (1956) experimental measurements on fracturing of a glass plate using spherical indenters of various radii. The measurement consisted of the load required for a sphere of a given size to produce a *hertzian cone* crack. If the indenter is pushed into the glass with a compressive force F then this load is reacted upon by a contact pressure along the surface of the sphere which is in contact with the glass. If P denotes the *mean contact pressure* then for equilibrium reasons we have

$$P = \frac{F}{\pi R^2} \tag{66}$$

where R is the radius of the circle at the intersection of the sphere and the planar surface of the glass. By virtue of the third of relationships (59)

$$P = \frac{2G\varepsilon_{\theta\theta}}{1 - \hat{\varepsilon}\hat{R}K_1(\hat{R})} \quad \text{at} \quad \hat{r} = \hat{R} \tag{67}$$

and by assuming that the breaking pressure is limited by the maximum extension strain $\varepsilon_{\theta\theta} = \varepsilon_c$ around the inflated hole, then the normalized *breaking force* f_{ef} is found to be

$$f_{\mathrm{ef}} = \frac{\hat{R}^2}{1 - \hat{\varepsilon}\hat{R}K_1(\hat{R})} \tag{68}$$

wherein

$$f_{\mathrm{ef}} = \frac{F_{\mathrm{ef}}}{2\pi G\ell^2\varepsilon_c} \tag{69}$$

and F_{ef} denotes the ultimate breaking force.

Tillet's experimental results that are also presented

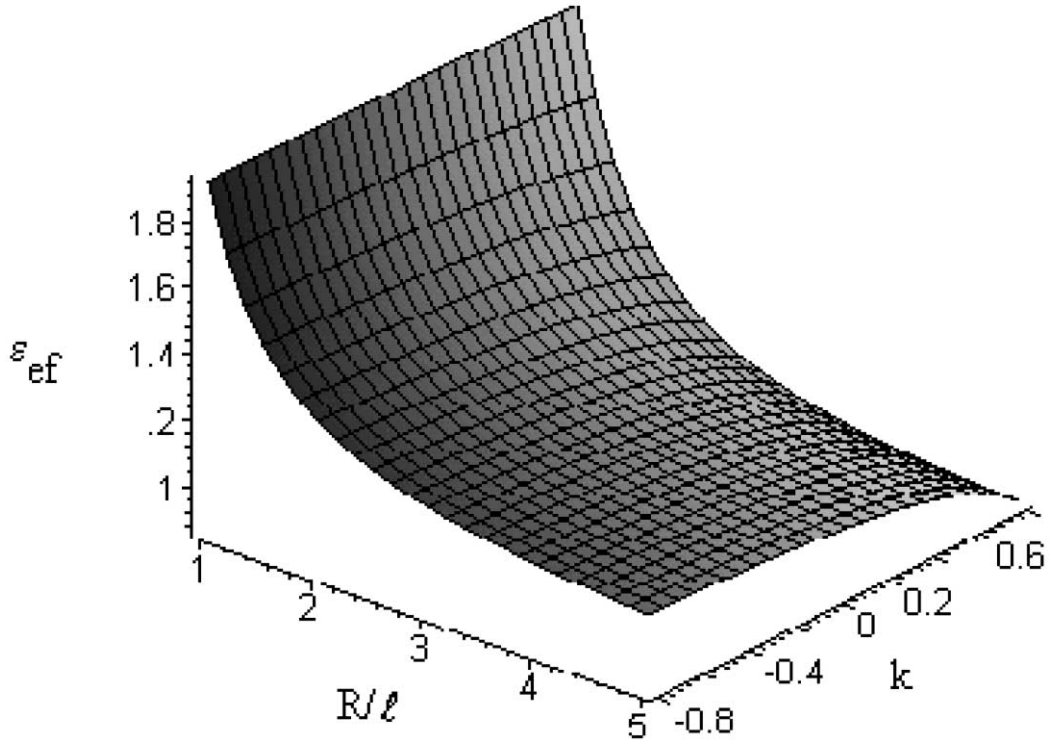

Fig. 6. Size effect exhibited by the uniformly pressurized elastic borehole for Poisson's ratio $\nu = 1/4$ and for various values of the ratio of surface length over the volume length, k.

graphically in Fig. 7, indicate that

$$F_{ef} = C_1 R^2 \quad \text{large } R,$$
$$F_{ef} = C_2 R \quad \text{small } R, \tag{70}$$

where C_1, C_2 are experimental constants. Tillet interpreted this experimental evidence by making the working hypothesis that in the interval of small sizes of radius where the law $F_{ef} = C_2 R$ is valid, the fracture occurs when the integrated energy exceeds some maximum, whereas in the region where $F_{ef} = C_1 R^2$ is valid, the fracture occurs when the stress (or strain) exceeds a maximum value. A more consistent interpretation of Tillet's experimental results, thus avoiding the assumptions of two failure criteria depending on the size of indenters, can be given by the present gradient-dependent elasticity theory. For this purpose a Taylor series asymptotic expansion of Eq. (68) around $\hat{R} = 1$ and $\hat{R} \to \infty$ is elaborated

$$f_{ef} = C_3 \hat{R} + O((\hat{R} - 1)^2),$$
$$\hat{R} \to 1, f_{ef} = \hat{R}^2, \quad \hat{R} \to \infty, \tag{71}$$

with C_3 to be constant that depends on Poisson's ratio ν and relative surface energy length$k$, respectively.

The variation of the normalized breaking force f_{ef} with normalized radius $\hat{R}$ as it is predicted by Eq. (68) is presented in Fig. 8. In the same figure the asymptotic curves predicted by Eq. (71) are also presented. As it can be seen in Fig. 8 the present gradient-dependent elasticity theory predicts nicely the deviation of the curve for small sizes of holes from the predictions of the classical elasticity theory, as it was observed in Tillet's experiments (Fig. 7). Thus, a unique opportunity is offered for the experimental determination in a non-destructive manner of lengths ℓ, ℓ' which are characteristic of material's microstructure. As it was demonstrated above this task can be achieved by

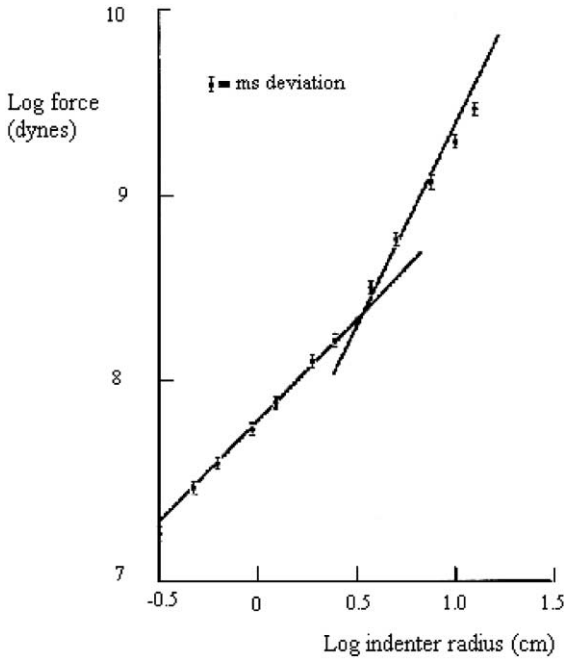

Fig. 7. Size effect exhibited by the breaking force in Tilett's indentation tests on glass plates (Tillet, 1956).

measuring the breaking force for various indenter radii through carefully performed non-destructive indentation tests, and then employing a back-analysis procedure to calibrate parameters ℓ, ℓ' such that to establish reasonable matching with experimental data. The estimated characteristic lengths of the material at hand, can then be used to simulate its behavior to various types of loading. In this manner, expensive, destructive laboratory tests for the determination of ℓ, ℓ' and the phenomena related with these lengths (e.g. boundary layer phenomena, size effect) may be avoided.

Next, another interpretation of indentation results will be given. For this purpose we introduce the mean dimensionless indentation radius as a strain-like measure

$$\varepsilon = \frac{\hat{R}}{\hat{\rho}} \tag{72}$$

in which $\hat{\rho}$ is the ratio of spherical indenter radius ρ over the intrinsic length scale ℓ. Identifying the strain ε with the hoop strain $\varepsilon_{\theta\theta}$ then Eq. (67) gives the pressure–strain relationship in indentation test. Fig. 9 shows the dependence of normalized indentation pressure on the normalized strain for three values of the relative surface energy length scale k at hand, and for $\nu = 1/4$. In the same figure the dashed line represents Hertz's solution

$$\hat{p} = \frac{P}{2G/\hat{\rho}} = \hat{\rho}\varepsilon \tag{73}$$

As we may see from Fig. 9 relationship (73) is valid for relatively large indentations and we may call it outer approximate solution. The inner solution which corresponds to relatively small indentations necessitates the enhancement of Eq. (73) so that singular terms in ε are included. In fact, it may be shown that the following asymptotic expansion of mean pressure for small strains is valid

$$\begin{aligned}\varepsilon_{\mathrm{ef}} = {} & \frac{2(1-2\nu)}{(1-2\nu)\{\log(2(\hat{\rho}\varepsilon)^{-1}) - \gamma\} + 1 - \nu}\,\frac{1}{\hat{\rho}\varepsilon} \\ & + k\,\frac{(1-2\nu)[\log(2(\hat{\rho}\varepsilon)^{-1}) - \gamma - (1-\nu)]}{\{(1-2\nu)\{\log(2(\hat{\rho}\varepsilon)^{-1}) - \gamma\} + 1 - \nu\}^2} \\ & + O(\hat{\rho}\varepsilon) \quad (\text{small } \varepsilon)\end{aligned} \tag{74}$$

The above inner solution has been also shown in Fig. 9 by a dashed line. From the same figure it is also noted that the effect of the surface energy on the pressure–strain relation is not significant. The same conclusion may be drawn from relation (74) where it is seen that the effect of k is of second order as compared to the effect of the volume-energy intrinsic length scale ℓ.

By setting the following definitions for the dimensionless load and radial displacement

$$\tilde{P} = \frac{P}{E/(1+\nu)}, \qquad \tilde{\delta} = \frac{u_r(R)}{R} \tag{75}$$

then by recourse to Eq. (58) we find the following relation

$$\tilde{P} = \varepsilon_{\mathrm{ef}}\tilde{\delta} \tag{76}$$

where $\varepsilon_{\mathrm{ef}}$ is given by Eq. (62). Hence, the total mechanical work $\mathrm{d}W$ done by the external pressure P in applying infinitesimal additional radial displacement $\mathrm{d}u_r$ is given by

$$\mathrm{d}W = \left(\int_0^{2\pi} PR\,\mathrm{d}\theta\right)\mathrm{d}u_r = 2\pi RP\,\mathrm{d}u_r \tag{77}$$

In view of relationship (77) and the first of Eq. (58) the total strain energy stored in the body will be given

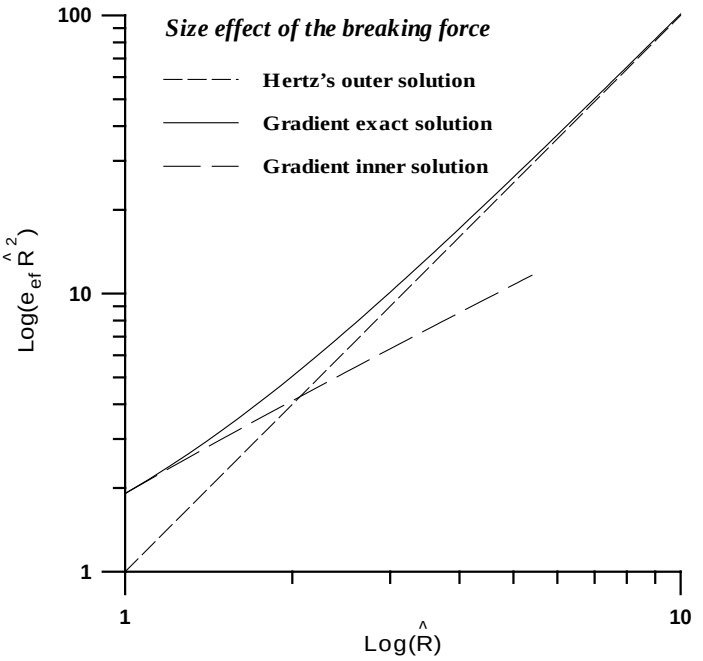

Fig. 8. Size effect in indentation (inflation) test predicted by gradient elasticity. Poisson's ratio $\nu = 1/4$ and relative surface energy parameter $k = 0$. Hertz's solution $(70)_1$ and asymptotic gradient solution $(71)_1$ are also displayed with dashed lines.

by

$$\tilde{W} = \pi R^2 \varepsilon_{\mathrm{ef}} \tilde{\delta}^2; \qquad \tilde{W} = \frac{W}{2G} \tag{78}$$

In order for the strain energy to be positive definite the following inequality must hold true

$$\varepsilon_{\mathrm{ef}} > 0 \tag{79}$$

Substituting in Eq. (79) the value of $\varepsilon_{\mathrm{ef}}$ as it given by Eq. (62) and based on the equality

$$\lim_{x\to\infty} \frac{K_{\mathrm{p}}(x)}{K_{\mathrm{q}}(x)} = 1$$

we finally derive the inequality that secures the positive-definiteness of W, namely

$$\frac{\ell'}{\ell} \leq 1 \tag{80}$$

Inequality (80) means that the case $\ell \neq 0, \ell' = 0$ is valid, while on the contrary the case $\ell = 0, \ell' \neq 0$ cannot exist since it results in negative definite strain energy density of the pressurized hole in an infinite plane configuration.

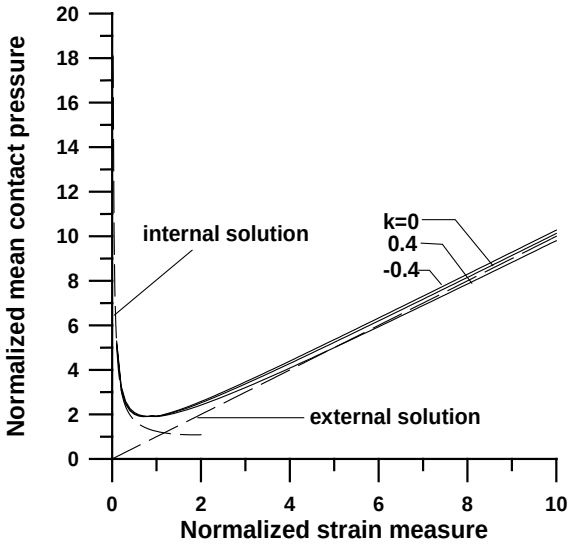

Fig. 9. Normalized mean contact pressure $\hat{p}$ vs. normalized strain $\hat{\rho}\varepsilon$ for $k = -0.4,\ 0,\ 0.4$, respectively, and $\nu = 1/4$. The dashed lines represent the classical Hertz's solution ("outer") and the singular gradient solution ("internal").

6. Strains and displacements in cracked solids

6.1. Introductory remarks

Professor G.I. Barenblatt (1962, p. 59) in his celebrated paper stated that: '…By using the model of an elastic body, we do not take into consideration all forces acting upon the body. It appears that for developing an adequate theory of cracks it is necessary to consider molecular forces of cohesion acting near the edge of a crack, where the distance between the opposite faces of the crack is small and the mutual attraction strong. Although consideration of forces of cohesion settles the matter in principle, it complicates a great deal the analysis. The difficulty is that neither the distribution of forces of cohesion over the crack surface nor the dependence of the intensity of these forces on the distance between the opposite faces are known. Moreover, the distribution of forces of cohesion in general depends on the applied loads…'. The first who introduced molecular forces of cohesion acting near the tip of a crack was Griffith who considered forces of cohesion as forces of surface tension being internal forces for the given body in order to develop his celebrated criterion of fracture mechanics (Griffith, 1921); however, their effect on the stresses and strains was neglected by Griffith. On the other hand, classical Linear Elastic Fracture Mechanics (LEFM) theory which was based on the concept of sharp Griffith cracks (considered as branch cuts) predicts infinite slope of the crack displacement at the crack tip. For example, for the specific case of mode-I deformation one can deduce

$$2G\frac{\partial \upsilon^{c}}{\partial x}(r,\pi) = -\sqrt{\frac{2}{\pi}}K_{I}\frac{(1-\nu)}{\sqrt{r}} \neq 2G\frac{\partial \upsilon^{c}}{\partial x}(r,0) = 0; \qquad r \to 0 \tag{81}$$

where the superscript 'c' denotes classical LEFM solution, (r,θ) are polar coordinates fixed at the crack tip, K_I is the mode-I stress intensity factor (SIF), and υ^c denotes the crack opening displacement. As it is shown in Fig. 10a the origin of the crack tip singularity lies in the fact that the originally sharp crack is widening due to the application of load into a parabolic tip (i.e.$\upsilon^c(r,\pi) \propto r^{1/2}$.) From a consideration of the term $\partial\upsilon^c/\partial x$, it is evident that the infinity in the slope is directly associated with the non-zero displacement at the very tip of the rounded crack. In his milestone paper in 1921 Griffith also proceeded to the investigation of the structure of the crack tip. This investigation was performed by Griffith without any consideration of cohesive forces, hence with infinite crack slope at the tip region. Griffith made an attempt to improve this description of the crack model by considering it as an elliptical cavity with a finite radius of curvature ρ at the tip (Fig. 10a). However, according to his estimate the magnitude of ρ was of the order of intermolecular distance, which, as it was pointed out by Barenblatt (1962), clearly indicates the contradiction with the original principle on which Griffith's derivation was based, that is, the continuous distribution of matter; in a continuous medium intermolecular distances cannot in principle be considered as finite.

Following a different approach Elliot (1947) proposed an atomistic model which explicitly accounted for the effect of the interatomic forces along the crack faces. An important result of this study was that the adjacent atomic planes defining the crack surface displace with respect to each other beyond the crack tip in contrast to the results of classical elasticity. Later Barenblatt (1959) in a celebrated work has introduced a small cohesive zone ahead of the 'physical' crack tip whose size is determined *explicitly* by requiring the cancellation of stress singularity at the tip of the cohesive zone (or tip of 'effective' crack), or equivalently smooth closure of crack lips. However, the slope of the crack opening displacement in mode-I deformation turns out to be infinite at the crack

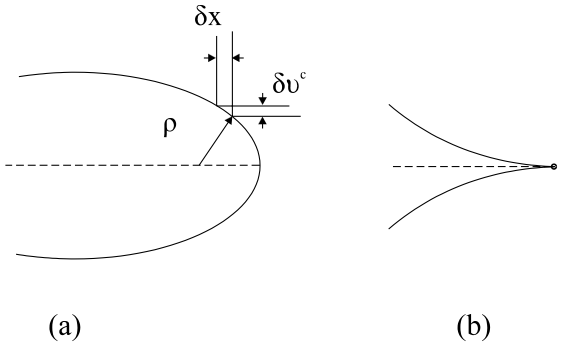

Fig. 10. (a) Classical model of crack tip. Originally branch cut (broken line) opens into rounded contour (full line). (b) Crack lips in the form of a cusp of the first kind with zero enclosed angle and zero first derivative of the displacement at the crack tip ($\partial\upsilon/\partial x = 0$).

tip/cohesive zone boundary, even though a smooth closure of crack lips is ensured (Fig. 10b). Indeed, Barenblatt (1959, p. 1013) gives the following expression for the mode-I crack opening displacement $v(x, y)$

$$v = \frac{\kappa + 1}{2G}\mathrm{Im}(\phi(\zeta)); \qquad \zeta = \mathrm{e}^{\mathrm{i}\theta} \tag{82}$$

withζ-values to correspond to the contour of the crack occupying the region $-\alpha \le x \le \alpha, y = 0^{\pm}$, i.e. the values $\zeta = \pm 1$ correspond to the crack tips. The complex function $\phi(\zeta)$ which assures finite stresses at the crack tips is given by

$$\phi(\zeta) = \frac{\alpha}{2\pi\mathrm{i}} \int_0^{\pi} g(\alpha\cos(\lambda))\sin(\lambda)\log\left(\frac{\zeta - \mathrm{e}^{\mathrm{i}\lambda}}{\zeta - \mathrm{e}^{-\mathrm{i}\lambda}}\right)d\lambda;$$

$$\lambda = \arccos\frac{x}{\ell} \tag{83}$$

and the distribution of stresses $g(x)$ to be determined by

$$g(x) = \begin{cases} p(x) - G(x) & \alpha \le x \le \alpha + d \\ p(x) & \alpha + d \le x \le -\alpha - d \\ p(x) - G(x) & -\alpha - d \le x \le -\alpha \end{cases} \tag{84}$$

In the above expressions (84) $p(x)$ is the intensity of the normal tensile stresses at the axis of symmetry, while $G(x)$ is the intensity of the cohesive forces and d is the width of the 'process zone'. By substituting Eqs. (84) and (83) into Eq. (82) and by performing an asymptotic analysis close to the crack tip we find

$$2Gv = (\kappa + 1)B\frac{\sin\theta}{(\cos\theta - 1)^2 + \sin^2\theta}, \qquad x \to \alpha^{-}; \tag{85}$$

$$B = \frac{\alpha}{3\pi}[p_0\pi^3 - G(\alpha)\lambda_0^3 - AG(\alpha)],$$

$$A = \pi^3 - (\pi - \lambda_0)^3,$$

$$p_0 = g(\alpha\cos\lambda), \qquad \lambda_0 = \sqrt{\frac{2d}{\alpha}}.$$

By differentiating Eq. (85) w.r.t. x one may easily obtain the result

$$2G\frac{\partial v}{\partial x} = \frac{(\kappa + 1)B\alpha}{2\sqrt{2}}(\alpha - x)^{-3/2} \qquad x \to \alpha^{-} \tag{86}$$

In addition, due to Eq. (86) the asymptotical value of the dislocation density as we approach the crack tip that is given by $\eta(x) = -\partial v/\partial x$ (Lardner, 1974) turns out to be infinite. Physically this is not possible, since dislocations cannot be less than a unit Burger's vector apart.

Sternberg and Muki (1967) have studied the Mode-I crack problem within the *linearized couple-stress theory* of elastic behavior. The problem was reduced to a system of two Fredholm integral equations of the second kind. It was found that the shape of the crack remains elliptical, as in the classical elasticity, and stress/strain inverse square-root singularities remain, although the detailed structure of the stress/strain field is altered. Later, Eringen, Spezialle and Kim (1977) have attacked the crack problem by using *non-local elasticity*. Their work seems to indicate that nonlocal elasticity eliminates the stress singularity at the crack tip; however, the solution seems to be approximate, in the sense that the stress boundary condition at the crack surface is not satisfied exactly.

Recently, Aifantis and co-workers (Altan and Aifantis, 1992; Aifantis, 1992; Altan and Aifantis, 1997) investigated the potential of applying gradient elasticity to crack problems which are considered as traction boundary value problems. For simplicity, Aifantis and co-workers studied only the effect of the volume energy strain gradient term ℓ whereas the concept of higher order self-equilibrating stresses μ_{ijk} doing work on higher order strain gradients was not introduced. It was found that this special theory leads to smooth closure of the crack outside the region occupied by the crack at infinity before the application of the load. However, the smooth closure of crack at infinity is an undesirable result of this type of formulation which may be seen in some sense as a constant load punch problem for a half-space.

6.2. Local solutions of mode-I, -II, -III crack problems

In this section the three basic crack deformation modes will be treated by employing the present anisotropic gradient elasticity theory with surface energy which is defined by Eq. (38)–(40). In contrast to Griffith's approach the effect of cohesive forces on the displacements and strains is considered in this theory by including higher order gradients in the constitutive equations.

Next, let us consider the *mixed-mixed* plane strain boundary value problems of a finite straight mode-I,

-II, and -III cracks occupying the line segment $-\alpha < x < \alpha, y = 0^{\pm}$ subjected to a uniform internal pressure $-\sigma_o$, with σ_o being a constant positive number, with no loading at infinity (Sternberg and Muki, 1967). Let S be the complement of the line segment $-\alpha < x < \alpha, y = 0$ extended on the half-plane $y \geq 0$. We seek the solution in S subject to the *mixed-mixed* boundary conditions derived directly from Eqs. (20) and (21). Vardoulakis et al. (1996); Exadaktylos (1997) have presented a methodology to reduce the above basic crack problems to a Fredholm integral equation of the second kind with a symmetric kernel.

According to the results presented in (Vardoulakis et al. (1996), Exadaktylos and Aifantis (1996) and Exadaktylos (1997) the crack shapes are no longer elliptical as predicted by LEFM but given by the formulae

$$\left.\begin{aligned} \upsilon(x,0^-) &= \ell \int_{\chi}^{\omega} \varphi^*(\ell\rho)\sqrt{\rho^2-\chi^2}\,d\rho, && \text{Mode-I} \\ u(x,0^-) &= \ell \int_{\chi}^{\omega} \psi^*(\ell\rho)\sqrt{\rho^2-\chi^2}\,\mathrm{d}\rho && \text{Mode-II} \\ w(x,0^-) &= \int_{\chi}^{\omega} \psi_3^*(\ell\rho)\sqrt{\rho^2-\chi^2}\,\mathrm{d}\rho && \text{Mode-III} \end{aligned}\right\} \quad (87)$$

where $\{\varphi^*(t),\ \psi^*(t),\ \psi_3^*(t)\}$ are continuous functions that depend on ℓ, ℓ', α and $\chi = x/\ell$. After integration by parts and an asymptotic analysis of the solution close to the crack tip (Vardoulakis et al., 1996; Exadaktylos, 1997; Vardoulakis and Exadaktylos, 1997), expressions (87) yield the following results

$$\left.\begin{aligned} \upsilon(r,0^-)\big|_{r\to 0} &= \frac{2\sqrt{2}}{3}\alpha^{1/2}\varphi^*(\alpha-\eta)r^{3/2} + o(r^{5/2}) && \text{Mode-I} \\ u(r,0^-)\big|_{r\to 0} &= \frac{2\sqrt{2}}{3}\alpha^{1/2}\psi^*(\alpha-\eta)r^{3/2} + o(r^{5/2}) && \text{Mode-II} \\ w(x,0^-)\big|_{r\to 0} &= \frac{2\sqrt{2}}{3}\alpha^{1/2}\psi_3^*(\alpha-\eta)r^{3/2} + o(r^{5/2}) && \text{Mode-III} \end{aligned}\right\} \quad (88)$$

where $r = \alpha - x$, and η is a small length (i.e. $\eta \ll \alpha$) which removes the weak logarithmic singularity of $\chi^*(t)$ at $t = \alpha$ for $k \neq 0$. According to Eq. (88) the mode-I, -II and -III crack shapes predicted by the present gradient elasticity theory are described by the equation

$$\left[\frac{x}{\alpha}\right]^2 + \left[\frac{d(x,0^-)}{\beta}\right]^{2/3} = 1, \quad (89)$$

$d(x,0^-) = \upsilon(x,0^-)$ or $u(x,0^-)$ or $w(x,0^-)$

where $\beta = d(0,0^-)$. That is, the crack lips form a *cusp* of the first kind with zero enclosed angle and zero first derivative of the displacement at the crack tip (Fig. 10b). This fact indicates that gradient elasticity theory predicts the same crack shape with Barenblatt's (1962) 'cohesive-zone' theory without requiring an extra assumption on the existence of interatomic forces at the outset beyond those implied by the gradient terms in the generalized constitutive equation.

Herein we compare the mode-III crack deformation solution predicted by the third of Eq. (87) with that given by Ru and Aifantis (1993). The Newmann expansion of the present solution for mode-III crack for zero value of the surface energy term, i.e. $k = 0$, yields

$$\begin{aligned} w(x,0) \approx \left(\frac{\sigma_0}{G}\right)\frac{\ell^{-8}}{5806080}\{ &-5083\alpha^6 + 1866x^2\alpha^4 \\ &-264x^4\alpha^2 + 16x^6 + 29376\ell^2\alpha^4 - 10368x^2\alpha^2\ell^2 \\ &+ 1152x^4\ell^2 - 169344\ell^4\alpha^2 + 48384x^2\ell^4 \\ &+ 967680\ell^6\}(\alpha^2 - x^2)^{3/2}, \end{aligned} \quad (90)$$

$$0 \leq x \leq \alpha, \qquad \frac{\ell}{\alpha} > \frac{1}{\sqrt{2}}$$

On the other hand Ru and Aifantis (R & A) solution in integral form along the crack surface is given by the formula

$$\begin{aligned} w(x,0) = &\left(\frac{\sigma_0}{G}\right) \\ &\times\left\{\frac{\mathrm{sh}\left(\dfrac{\alpha+x}{\ell}\right)}{\ell\,\mathrm{sh}\left(\dfrac{2\alpha}{\ell}\right)}\int_{-\alpha}^{\alpha}\mathrm{sh}\left(\frac{\alpha-t}{\ell}\right)\sqrt{t^2-\alpha^2}\,\mathrm{d}t\right. \\ &\left. -\frac{1}{\ell}\int_{-\alpha}^{x}\mathrm{sh}\left(\frac{x-t}{\ell}\right)\sqrt{t^2-\alpha^2}\,\mathrm{d}t\right\} \end{aligned} \quad (91)$$

Fig. 11 shows the semi-crack profiles predicted by the above solutions (90) and (91), respectively. It is

seen that the second solution predicts a wedge-shaped crack tip with a finite angle in contrast to the proposed gradient solution which results in a cusp-shaped crack tip region as is also predicted by asymptotic expansions (88). Furthermore, Fig. 12 depicts the ratio of mode-III crack displacement at centre of the crack to the corresponding classical value as a function of the dimensionless volume energy term ℓ/α in the absence of surface energy predicted by R & A and the present gradient formula (87), 3. The 'cross' symbols correspond to the numerical solution of the Fredholm integral equation of the second kind corresponding to the mode-III crack. Also, in the same figure we have plot the following approximate representation of R & A integral expression (91) that is valid for large values of the relative volume energy term ℓ/α

$$w(0,0) \approx \left(\frac{\sigma_0}{G}\right)\left(\frac{\pi\alpha}{2}\right)\left[\left\{\frac{1}{2} - \frac{2}{3\pi}\right\}\left(\frac{\alpha}{\ell}\right)^2 - \left\{\frac{5}{48} + \frac{2}{45\pi}\right\}\left(\frac{\alpha}{\ell}\right)^4\right] + O\left[\left(\frac{\alpha}{\ell}\right)^6\right] \tag{92}$$

From Fig. 12 we may infer that both gradient solutions tend to the classical prediction for $\ell/\alpha \to 0$ and the crack displacement diminishes monotonically, or alternatively the crack becomes 'stiffer' in comparison to the classical LEFM displacement, as the relative volume energy term increases. The first observation corrects the assertion made in (Vardoulakis et al., 1993), namely that R & A solution tends to a higher value of crack diplacement than that predicted by LEFM as $\ell/\alpha \to 0$. The second observation is due to the fact that the consideration of forces of cohesion in both gradient theories always leads to lower displacements that those predicted by the classical theory which does not consider such forces.

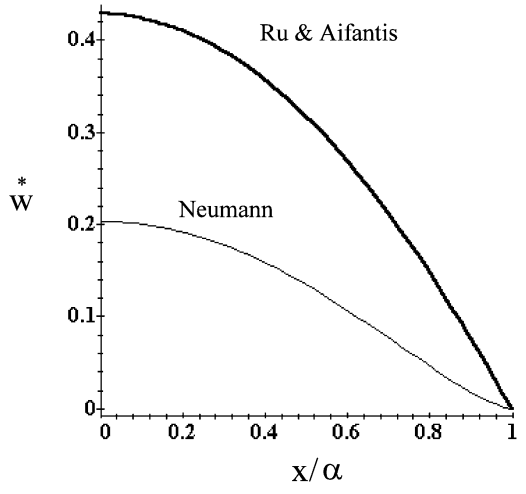

Fig. 11. Mode-III crack profiles predicted by Ru and Aifantis solution (91) and by the present Neumann solution (90) for $\ell/\alpha = 0.8$, $\alpha = 1$, $k = 0$, and $w = w(x,0)/(\sigma_0/G)$.

Next, let $\bar{S}$ from here on stand for the open half-plane $y \le 0$ together with its bounding edge, i.e. for the region $(-\infty < y \le 0,\ -\infty < x < \infty)$. Introducing polar coordinates r_1, θ_1, r, θ, r_2, θ_2, as it is shown in Fig. 13, through the relations

$$z = r\,e^{i\theta},\ z - \alpha = r_1\,e^{i\theta_1},\ z + \alpha = r_2\,e^{i\theta_2} \tag{93}$$

we seek to determine the behavior of the mode-I, -II, -III gradient elasticity solutions at the endpoints of the crack. We obtain the following asymptotic estimate for the displacements of the three basic modes, which holds true as $r_1 \to 0$ for every fixed positive ℓ

$$2G\upsilon(r_1,\theta_1) = S\sqrt{2\alpha}r_1^{1/2}\sin\frac{\theta_1}{2}\cos^2\frac{\theta_1}{2} - \frac{2}{3}S\sqrt{2\alpha}\varphi^*(\alpha-\eta)r_1^{3/2}\sin\frac{3\theta_1}{2} + o(r_1^{5/2}) \quad \text{Mode-I}$$

$$2Gu(r_1,\theta_1) = S\sqrt{2\alpha}r_1^{1/2}\sin\frac{\theta_1}{2}\cos^2\frac{\theta_1}{2} - \frac{2}{3}S\sqrt{2\alpha}\psi^*(\alpha-\eta)r_1^{3/2}\sin\frac{3\theta_1}{2} + o(r_1^{5/2}) \quad \text{Mode-II}$$

$$2Gw(r_1,\theta_1) = -\frac{2}{3}S\sqrt{2\alpha}\psi_3^*(\alpha-\eta)r_1^{3/2}\sin\frac{3\theta_1}{2} + o(r_1^{5/2}) \quad \text{Mode-III} \tag{94}$$

where throughout this paper the order-of-magnitude symbols 'O' and 'o' are used in their standard mathematical connotation (Erdélyi, 1956); in particular, a function is $O(1)$ if it remains bounded in the underlying limit, whereas it is $o(1)$ if it vanishes in the underlying limit.

The first derivative of the crack displacement with respect to x near the crack tip (i.e. the slope of the crack profile) for each one of the basic crack modes

can be found from Eq. (94) to be

$$2G\frac{\partial v}{\partial x}(r_1,\theta_1)=S\frac{\sqrt{2\alpha}}{4}r_1^{-1/2}\sin\theta_1\cos\frac{\theta_1}{2}\left\{\cos\theta_1-2\left[\cos^2\frac{\theta_1}{2}-2\sin^2\frac{\theta_1}{2}\right]\right\}+S\sqrt{2\alpha}\varphi^*(\alpha-\eta)r_1^{1/2}\times\left\{\sin\theta_1\cos\frac{3\theta_1}{2}-\cos\theta_1\sin\frac{3\theta_1}{2}\right\}+o(r_1^{3/2})\quad\text{Mode-I}$$

$$2G\frac{\partial u}{\partial x}(r_1,\theta_1)=S\frac{\sqrt{2\alpha}}{4}r_1^{-1/2}\sin\theta_1\cos\frac{\theta_1}{2}\left\{\cos\theta_1-2\left[\cos^2\frac{\theta_1}{2}-2\sin^2\frac{\theta_1}{2}\right]\right\}+S\sqrt{2\alpha}\psi^*(\alpha-\eta)r_1^{1/2}\times\left\{\sin\theta_1\cos\frac{3\theta_1}{2}-\cos\theta_1\sin\frac{3\theta_1}{2}\right\}+o(r_1^{3/2})\quad\text{Mode-II}$$

$$2G\frac{\partial w}{\partial x}(r_1,\theta_1)=S\sqrt{2\alpha}\psi_3^*(\alpha-\eta)r_1^{1/2}\times\left\{\sin\theta_1\cos\frac{3\theta_1}{2}-cos\theta_1\sin\frac{3\theta_1}{2}\right\}+o(r_1^{3/2})\quad\text{Mode-III}\tag{95}$$

From the above formula it is interesting to find the values of the slope in front and behind the crack tip for the three modes

$$2G\frac{\partial d}{\partial x}=\begin{cases}0 & \theta_1=0\\ -S\sqrt{2\alpha}\chi^*(\alpha-\eta)r_1^{1/2} & \theta_1=\pi\end{cases}\tag{96}$$

where the function $\chi^*(\cdot)$ takes the values $(\varphi^*(\cdot),\psi^*(\cdot),\psi_3^*(\cdot))$, respectively, and d is defined in Eq. (89). Hence, another important and new result is that the present gradient-dependent elasticity theory predicts-in contrast to LEFM-that the slope of the crack displacement for the three modes is *finite* and *continuous*, i.e.

$$\lim_{x\to\alpha^-}\frac{\partial d}{\partial x}(x,0^-)=\lim_{x\to\alpha^+}\frac{\partial d}{\partial x}(x,0^-)=0\tag{97}$$

On the contrary, as it was shown above R & A solution predicts a wedge-shaped crack tip with finite angle, hence the strain at crack tip is nonzero. In fact from formula (91) it is found

$$\left.\frac{dw}{dx}\right|_{x=-\alpha}=\frac{\sigma_0}{G}\frac{1}{\ell^2\,\mathrm{sh}\left(\frac{2\alpha}{\ell}\right)}\times\int_{-\alpha}^{\alpha}\mathrm{sh}\left(\frac{\alpha-t}{\ell}\right)\sqrt{\alpha^2-t^2}\,dt;\quad y=0\tag{98}$$

It is also noted that the finite derivative come from the first integral of Eq. (91) whereas the second integral gives a cusping crack. Fig. 14 also illustrates the dependence of the strain at crack tip on the relative micromaterial length scale ℓ/α which is predicted by R & A integral representation Eq. (98). The above observation, namely of the finiteness of the strain at crack tip, leads to the direct conclusion that R & A solution predicts that the first derivative of the displacement on the crack plane ($y=0$) with respect to x is discontinuous. Explicitly

$$\lim_{x\to-\alpha^-}\frac{\partial w}{\partial x}(x,0^+)=0\neq\lim_{x\to-\alpha^+}\frac{\partial w}{\partial x}(x,0^+)=C\neq0\tag{99}$$

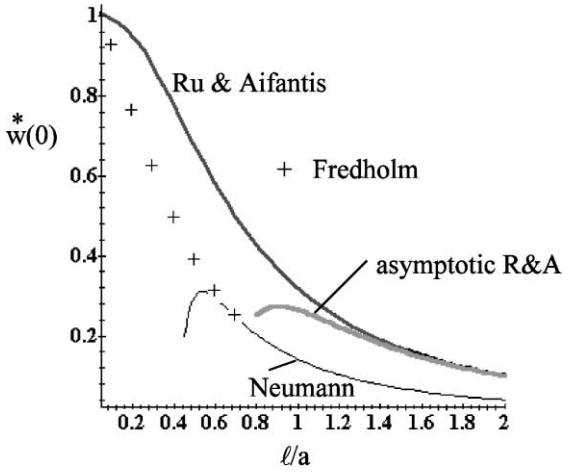

Fig. 12. Comparison of the Mode-III crack displacement at centre of mode-III crack as a function of the dimensionless volume energy term predicted by R & A solution (91) and by the present solution for $k=0$, and $w=w(x,0)/(\sigma_0/G)$. The Newmann asymptotic expansion of the present gradient solution is given by Eq. (90) whereas the asymptotic solution of R & A is given by Eq. (92).

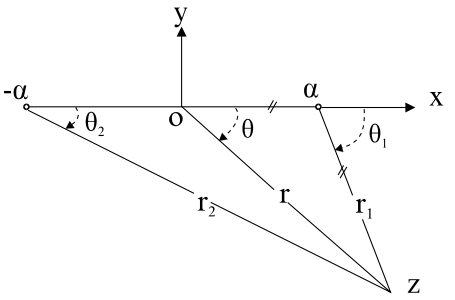

Fig. 13. Crack and coordinates.

hence the crack profile predicted by the same solution is physically unrealistic.

In the context of the proposed theory the energy release during an infinitesimal advancement of the crack tip by a distance $\delta\alpha$ can be found to be

$$\delta U = G_a \delta\alpha = \int_0^{\delta\alpha} \sigma(\delta\alpha - h, 0+)\, \mathrm{d}(h, -\pi)\, \mathrm{d}h$$

$$= \frac{K_a^2}{8G}\chi^*(\alpha - \eta)(\delta\alpha)^2, \quad \delta\alpha \to 0 \tag{100}$$

where $\sigma = \{\sigma_{yy}, \sigma_{xy}, \sigma_{yz}\}$ is the nominal stress for each basic crack deformation mode, $K_a = \sigma_0\sqrt{\pi\alpha}$ is the corresponding SIF and G_a (a = I,II,III) is the relevant crack-extension force. It should be mentioned that Barenblatt's and Dugdale's stress-finiteness condition for elastic-brittle and elasto-plastic fracture, respectively, results to a similar dependence as that given by Eq. (100), i.e. $G_a \propto \delta\alpha$, $\delta\alpha \to 0$, with the immediate consequence that the energy release rate turns out to approach zero for an infinitesimal crack extension. Barenblatt (1962) called this type of cracks 'equilibrium cracks', i.e. cracks for which the energy released by a very small change in the shape of the crack is equal to zero.

In view of the above result the criterion for crack growth should be stated as follows (Exadaktylos, 1997)

$$G_a \geq \beta\ \delta\alpha; \qquad (a = I, II, III) \tag{101}$$

where $\delta\alpha$ is the minimum crack extension length such that the above inequality holds true. The quantity β called herein 'modulus of cohesion', has the dimensions of energy per unit volume, and it is a fundamental property of the material with microstructure. Thus the 'specific fracture energy' with dimensions $[\gamma] = FL^{-1}$ has to depend linearly on $\delta\alpha$ for crack tip propagation distances that are not large as compared to the structure of the elastic-perfectly brittle material, that is,

$$\gamma = \gamma(\delta\alpha) = \beta\delta\alpha \ \text{ as } \ \delta\alpha \to 0 \tag{102}$$

Definition (102) is in agreement with the experimental results of Hoagland et al. (1973) who found that the specific fracture energy or fracture resistance of Salem limestone was an increasing function of crack propagation distance at an early stage of crack extension, but finally reached asymptotically a constant value corresponding to large—relative to the grain size—pre-existing flaws in the rock (Fig. 15). γ-curve, i.e. the curve of γ as a functon of $\delta\alpha$, must start from zero as indicated in Eq. (102); at zero stress the size of the process zone is zero — it requires no energy to form a process or microcraking zone of zero size.

By virtue of definition (102), Griffith's rupture criterion is modified as follows

$$X(\alpha - \eta; \ell, \ell') \geq \beta,$$

$$X(\alpha - \eta; \ell, \ell') = \frac{\pi\alpha}{8}\frac{\sigma_0^2}{G}\chi^*(\alpha - \eta) \tag{103}$$

$$= \frac{K_a^2}{8G}\chi^*(\alpha - \eta)$$

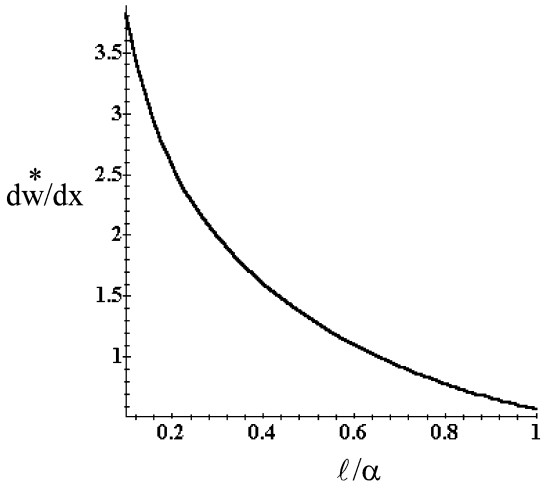

Fig. 14. Plot of normalized slope at crack tip $\mathrm{d}\overset{*}{w}/\mathrm{d}x$ vs. relative volume energy intrinsic length scale ℓ/α derived from R & A integral representation (98).

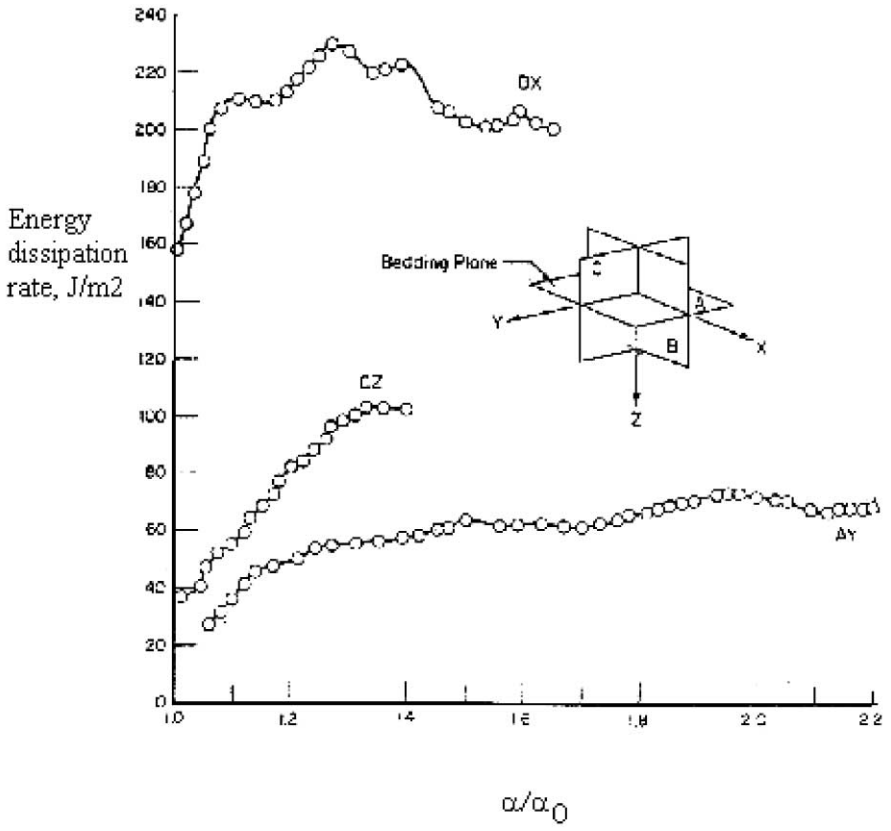

Fig. 15. Energy dissipation rates measured over an interval of crack length for three orientations of the crack plane and propagation direction in Salem limestone. The letters A, B, and C denote orientation of the crack plane with respect to the bedding (A) and *X*,*Y*,*Z* denote crack propagation direction. α/α_0 is the ratio of crack length to the starting slot length (Hoagland et al., 1973).

where the function X in Eq. (103) depends on the applied pressure on the faces of the crack, on crack length and on material length parameters ℓ, ℓ'. The corresponding critical value of K_a ($a = \mathrm{I,II,III}$) which represents the fracture resistance of the material is denoted by K_{aC} and is called 'fracture toughness' or 'critical stress intensity factor'. Note from Eq. (103) that

$$K_{\mathrm{IC}} = \sqrt{\frac{8\beta G}{\varphi^*(\alpha - \eta)}} \tag{104}$$

The variation of the normalized K_{IC} with the ratio α/ℓ is depicted in Fig. 16 for three values of the material length ratio, namely for $k = \ell'/\ell = -0.2$, 0, and 0.2, and for Poisson's ratio $\nu = 0.25$. It can be seen that the resistance to fracture of the material decreases with increasing relative crack size; positive values of the surface energy parameter ℓ' further enhance the strength of the material, whereas negative values of the surface energy parameter lead to a decrease of the fracture toughness of the material. The previous result of gradient elasticity theory agrees qualitatively with experimental results which indicate that materials with *smaller* cracks are more resistant to fracture than those with *larger* cracks. It is important to mention here that classical LEFM does not predict an effect of the size of the crack on K_{aC}, that is, it considers it as a constant.

If the classical fracture criterion in plane strain conditions

$$\frac{(1-\nu^2)}{E} K_I^2 \geq 2\gamma \tag{105}$$

were used to compute the critical energy release rate

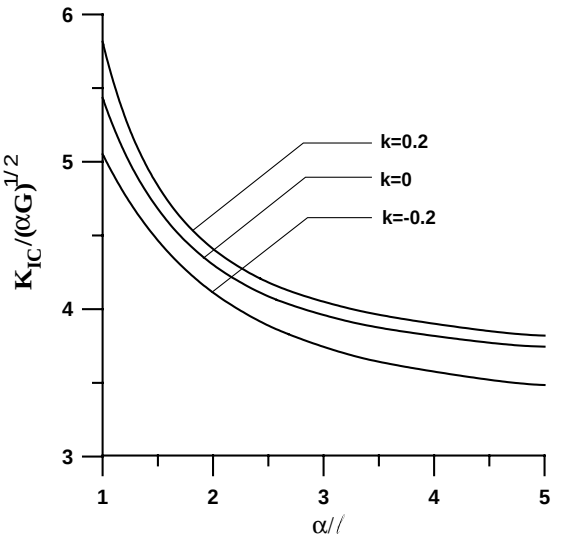

Fig. 16. Size effect of the normalized K_{IC} for three values of the material length ratio $k = \ell'/\ell$ and for Poisson's ratio of the material $\nu = 1/4$.

G_{IC} from the critical stress intensity factor K_{IC}, the value of G_{IC} so determined would be several orders of magnitude greater than the surface energy 2γ. Or, conversely, if G_{IC} were equated to the surface energy, then unrealistically small failure loads would be predicted for the material under investigation. The investigation of the applicability of the Griffith–Irwin criterion (105) to the fracture of real solids is displayed in Table 1 and it was presented by Lawn and Wilshaw (1975). Based on the data presented in this table, Lawn and Wilshaw commented that:'… *energy dissipation processes other than those involved in mere surface formation operate at crack tips in certain solids* ($G_c \gg 2\gamma$)…'. However, it can be demonstrated (Vardoulakis et al., 1996; Exadaktylos, 1997) that the modified fracture criterion (101) based on the consideration of higher order gradients and double stresses predicts physically reasonable surface energy and failure stress values for appropriate values of the parameters ℓ, ℓ', β, hence we do not need to introduce *ad hoc* assumptions of the *Irwin–Orowan* type in order to capture this observed discrepancy of the energy dissipation at the crack tip.

Performing mode-I fracture mechanics experiments on brittle specimens with known shear modulus G one then can estimate the critical K_{IC} and the modulus of cohesion β from the slope of the specific fracture energy 2γ against crack length. Accordingly, the characteristic material lengths ℓ, ℓ' can be estimated from the size effect exhibited by K_{IC} (e.g. Fig. 16).

From condition (175) for the onset of crack extension a first order approximation of the breaking stress σ_t for $\ell' = 0$ can be obtained as follows (Exadaktylos, 1997)

$$\sigma_t \cong \sqrt{\frac{8E\beta}{\pi(1-\nu^2)}}\frac{\ell}{\alpha} + O\left(\left[\frac{\ell}{\alpha}\right]^2\right) \tag{106}$$

In classical elasticity $\sigma_t \propto \alpha^{-1/2}$ and clearly if α is small enough σ_t may have to exceed the yield strength of the material in order to initiate cracks. Thus, in terms of classical elasticity we imply the existence of a limiting crack size 'α' below which sharp crack fracture mechanics will not apply. On the other hand, gradient elasticity has no such restriction, since as it can be seen from (178) for any value of α whatever small, the characteristic length scale of the discrete structure of the material ℓ should be sufficiently small at that scale in order for the stress not to exceed the yield strength of the material at hand.

Furthermore, the above inverse first-power dependence of strength on the size of the crack-like defect agrees with the experimental results on elastomers presented by Bueche and Berry (1959). The relation between the depth of the surface cut and tensile strength for a polymer found by Bueche and Berry is displayed in the log–log diagram of Fig. 17. The solid line is of unit slope (i.e. $\sigma_t \propto \alpha^{-1}$) and gives a fair agreement with the experimental points, although of course the scatter is considerable. On the other hand, Griffith's criterion predicts an inverse square-root relation, so it does not give the correct dependence of the tensile strength on the size of the pre-existing crack. It is to be expected that the above modified rupture criterion proposed herein, will not apply quantitatively to rubbery materials, but dimensional requirements indicate that the above dependence of strength on cut size should be a good approximation.

7. Conclusions

The following conclusions can drawn at once from the series of rock mechanics and rock fracture mechanics examples dealt with in the foregoing

Table 1
Computed surface energy ($2\gamma \approx 2Eb_0/\pi^2$) and measured crack-extension force (G_c) for various material classes and for single crystal materials under plane strain, environment-free conditions (Lawn and Wilshaw, 1975) (E = Young's modulus, b_0 = spacing between separating molecular units). Bold typed entries mark the cases in which $G_c \gg 2\gamma$.

Class	Material	Cleavage	E (GPa)	b_0 (nm)	2γ (J/m^2)	G_c (J/m^2)
Covalent	C (diamond)	Diamond (111)	1000	0.15	30	–
	Si	Diamond (111)	130	0.24	6.2	3
	Ge	Diamond (111)	100	0.25	5.0	2
Covalent-ionic	Al_2O_3		350	0.19	13.4	7
	SiO_2 (quartz)	No preferred cleavage	80	0.16	**2.6**	**20**
	SiO_2(fused silica)		72	0.16	**2.4**	**9**
	Soda-lime glass		72	0.16	**2.4**	**8**
Ionic	MgO	NaCl (100)	240	0.21	10.0	3
	LiF	NaCl (100)	91	0.20	3.6	0.8
	NaCl	NaCl (100)	43	0.28	2.4	0.6
	Mica	Basal (0001)	200	0.14	**5.6**	**10**
Metallic	W	bcc (100)	390	0.27	22	3
	a-iron (steel)	bcc (100)	200	0.25	**10.0**	$\mathbf{2\times10^3}$
	Zn	hcp (0001)	120	0.27	6.4	0.2
	Be	hcp (0001)	300	0.23	14	$\mathbf{1\times10^3}$
Polymeric	PMMA	No preferred cleavage	2	1	0.4	$\mathbf{4\times10^2}$

sections. First, it was demonstrated by virtue of a simplified 1D geometry of the tension test that the present 2nd gradient theory predicts non-linear variation of the displacement field even though the applied surface tractions are uniform. Also it was shown for both the tension test and axisymmetric borehole configurations that the strength of the materials with structure is a function of the ratio h/ℓ where h is the characteristic dimension of the material under investigation. The surface energy length scale ratio ℓ'/ℓ depicts the intensity of the size effect due to surface stress phenomena. Next, the basic static crack

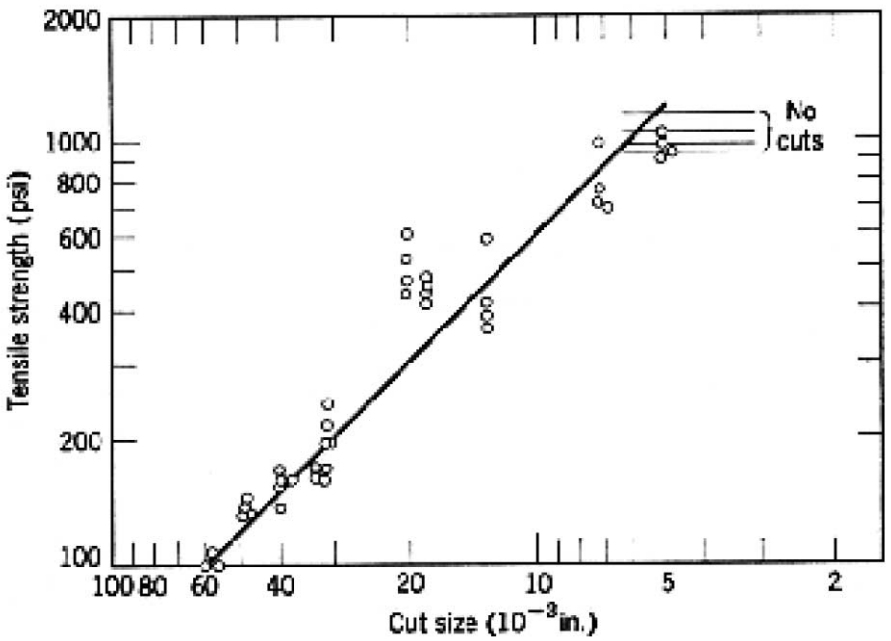

Fig. 17. The relation between cut (artificial defect) size and tensile strength of a filled vulcanized silicone elastomer (Bueche and Berry, 1959).

problems have been investigated in the context of the proposed gradient elasticity theory that have direct practical applications in the theory of strength of materials and mechanics of earthquakes in the earth's crust. It was illustrated that the solution of these three basic crack deformation modes leads to cusping of the crack tips that is caused by the action of "cohesive" double forces behind and very close to the tips, that tend to bring the two opposite crack lips in close contact. Furthermore, it was demonstrated that the fracture toughness depends on the size of the crack, and thus it is not a fundamental property of the material. This latter outcome agrees with experimental results which indicate that materials with smaller cracks are more resistant to fracture than those with larger cracks. Hence, the proposed *nonlocal* theory allows the rock mechanics and rock fracture mechanics problems to be described with a degree of physical insight, simplicity and exactness hitherto unknown.

Acknowledgements

This article is a partial result of research supported by funds of the GSRT of Hellas through the programme PENED 99 ED 642. Finally, the authors would like to dedicate this work to Professor Bruce Hobbs for his significant contribution to Earth Sciences.

References

Altan, B., Aifantis, E.C., 1992. On the structure of the mode III crack-tip in gradient elasticity. Scripta Met. 26, 319.

Altan, B., Aifantis, E.C., 1997. On some aspects in the special theory of gradient elasticity. J. Mech. Beh. Mater. 8 (3), 231–282.

Aifantis, E.C., 1992. On the role of gradients in the localization of deformation and fracture. Int. J. Engng. Sci. 30, 1279.

Barenblatt, G.I., 1959. Equilibrium cracks formed during brittle fracture — Rectilinear cracks in plane plates. J. Appl. Math. Mech. 23, 1009–1029.

Barenblatt, G.I., 1962. Mathematical theory of equilibrium cracks in brittle fracture. Adv. Appl. Mech. 7, 55.

Bazant, Z.P., Cedolin, L., 1991. Stability of Structures: Elastic Inelastic, Fracture, and Damage Theories. Oxford University, NY.

Bueche, A.M., Berry, J.P., 1959. The mechanisms of polymer failure. Fracture. In: Proceedings Internationl Conference on the Atomic Mechanisms of Fracture, pp. 265–353.

Casal, P., 1961. La capillarite interne. Cahier du Groupe Francais d'Etudes de Rheologie C.N.R.S. VI (3), 31–37.

Casal, P., 1963. Capillarite interne en mecanique. C.R. Acad. Sci. 256, 3820–3822.

Casal, P., 1972. La theorie du second gradient et la capillarite. C.R. Acad. Sci. A (274), 1571–1574.

Cosserat, E., Cosserat, F., 1909. Theorie de Corps Deformables. In: Hermann, A. (Ed.), Paris.

Elliot, H.A., 1947. An analysis of the conditions for rupture due to Griffith cracks. Proc. Phys. Soc. 59, 208–223.

Erdelyi, A., 1956. Asymptotic Expansions. Dover Publications , NY.

Eringen, A.C., Speziale, C.G., Kim, B.S., 1977. Crack-tip problem in non-local elasticity. J. Mech. Phys. Solids 25, 339–355.

Eshelby, J.D., 1951. The force on an elastic singularity. Phil. Trans. R. Soc. Lond. A 244 (877), 87–112.

Exadaktylos, G.E., 2001. Gradient elasticity with surface energy: Mode-I crack problem. Int. J. Solids Struct. (in press).

Exadaktylos, G.E., Aifantis, E.C., 1996. Two and three dimensional crack problems in gradient elasticity. J. Mech. Beh. Mtls. 7 (2), 93–117.

Germain, P., 1973a. La methode des puissances vituelles en mecanique des milieux continus Part I. J. Mec. 12, 235–274.

Germain, P., 1973b. The method of virtual power in continuum mechanics Part 2: Microstructure, SIAM. J. Appl. Math. 25, 556–575.

Griffith, A.A., 1921. The phenomena of rupture and flow in solids. Phil. Trans. R. Soc. Lond. A 221, 163.

Hoagland, R.G., Hahn, G.T., Rosenfield, A.R., 1973. Influence of microstructure on fracture propagation in rock. Rock Mech. 5, 77.

Kröner, E. (Ed.), 1967. Mechanics of generalized continua. Proceedings of the IUTAM — Symposium of The Generalized Cosserat Continuum and the Continuum Theory of Dislocation With Applications, Freudenstadt and Stuttgart (Germany).

Lardner, R.W., 1974. Mathematical Theory of Dislocations and Fracture. University of Toronto Press, Toronto.

Lawn, B.R., Wilshaw, T.R., 1975. Fracture of Brittle Solids. Cambridge University Press, Cambridge.

Love, A.E.H., 1927. A treatise on the mathematical theory of elasticity. Cambridge.

Mindlin, R.D., 1964. Micro-structure in linear elasticity. Arch. Rational Mech. Anal. 16, 51.

Mindlin, R.D., 1965. Second gradient of strain and surface-tension in linear elasticity. Int. J. Solids Struct. 1, 417.

Mindlin, R.D., Eshel, N.N., 1968. On first strain-gradient theories in linear elasticity. Int. J. Solids Struct. 1, 109–124.

Muhlhaus, H.B., Vardoulakis, I., 1987. The thickness of shear bands in granular materials. Geotechnique 37, 271–283.

Muhlhaus, H.B., deBorst, R., Sluys, L.J., Pamin, J., 1994. A thermodynamic theory for inhomogeneous damage evolution. In: Siriwardane, Zaman (Eds.). Computational Methods and Advances in Geomechanics. Balkema, pp. 635–640.

Muskhelishvili, N.I., 1963. In: Noordhoff, P. (Ed.). Some basic problems of the mathematical theory of elasticity. Groningen.

Norbury, J., Wheeler, A.A., 1987. On the penetration of an elastic-plastic material by a slender body. Q. J. Mech. Appl. Math. 40 (4), 477–491.

Pettofrezzo, A.J., 1978. Matrices and Transformations. Dover Publications, NY.

Ru, C.Q., Aifantis, E.C., 1993. A simple approach to solve boundary-value problems in gradient elasticity. Acta Mech. 101, 59.

Stacey, T.R., 1981. A simple extension strain criterion for fracture of brittle rock. Int. J. Rock Mech. Min. Sci. Geomech. Abstr. 18, 469–474.

Sternberg, E., Gurtin, M.E. 1962. On the completeness of certain stress functions in the linear theory of elasticity. In: Proceedings of.the fourth US Nation. Congress Applied Mech., University of California, Berkeley, ASME, NY.

Sternberg, E., Muki, R., 1967. The effect of couple-stresses on the stress concentration around a crack. Int J. Solids Struct. 3, 69–95.

Tillet, J.P.A., 1956. Proc. Phys. Soc. Lond. B 69, 47.

Toupin, R.A., 1962. Elastic materials with couple-stresses. Arch. Ration. Mech. Anal. 11, 385–414.

Vardoulakis, I., 1997. Lecture notes on 'Behavior of granular materials':Strain localization in granular materials. (Editor Bernard Cambou) CISM Lecture Notes.

Vardoulakis, I., Exadaktylos, G.E., 1997. The asymptotic solution of anisotropic gradient elasticity with surface energy for a mode-II crack. Non-linear singularities in deformation and flow. In: Durban, D., Pearson, J.R.A., (eds.), IUTAM Symposium, Haifa, Israel.

Vardoulakis, I., Sulem, J., 1995. Bifurcation Analysis in Geomechanics. Blackie Academic and Professional.

Vardoulakis, I., Exadaktylos, G., Aifantis, E., 1996. Gradient elasticity with surface energy: Mode-III crack problem. Int. J. Solids Struct. 33 (30), 4531–4559.

Voigt, W., 1887. Theoretische Studien ueber die Elastizitaetverhaeltnisse der Krystalle. Adh. Ges. Wiss. Gottingen, vol. 34 (1894). Uber Medien ohne innere Krafte und eine durch sie gelieferte mechanische Deutung der Maxwell-Hertzcshen Gleichungen. Gott. Abh.1894 72–79

Watson, G.N., 1966. Theory of Bessel Functions. Cambridge University Press.

Wu, C.H., 1992. Cohesive elasticity and surface phenomena. Q. Appl. Math. L 1, 73–103.